Integrated investment, retrofit and abandonment planning of energy systems with short-term and long-term uncertainty using enhanced Benders decomposition

Hongyu Zhang[a,*], Ignacio E. Grossmann[b], Brage Rugstad Knudsen[d], Ken McKinnon[1], Rodrigo Garcia Nava[1], Asgeir Tomasgard[a]

[a] *Department of Industrial Economics and Technology Management, Norwegian University of Science and Technology, Høgskoleringen 1, 7491, Trondheim, Norway*
[b] *Department of Chemical Engineering, Carnegie Mellon University, 5000 Forbes Avenue, Pittsburgh, PA 15213, USA*
[c] *SINTEF Energy Research, Kolbjørn Hejes vei 1B, 7491, Trondheim, Norway*
[d] *School of Mathematics, University of Edinburgh, James Clerk Maxwell Building, Peter Guthrie Tait Road, Edinburgh, EH9 3FD, United Kingdom*

Abstract

We propose the REORIENT (REnewable resOuRce Investment for the ENergy Transition) model for energy systems planning with the following novelties: (1) integrating capacity expansion, retrofit and abandonment planning, and (2) using multi-horizon stochastic mixed-integer linear programming with short-term and long-term uncertainty. We apply the model to the European energy system considering: (a) investment in new hydrogen infrastructures, (b) capacity expansion of the European power system, (c) retrofitting oil and gas infrastructures in the North Sea region for hydrogen production and distribution, and abandoning existing infrastructures, and (d) long-term uncertainty in oil and gas prices and short-term uncertainty in time series parameters. We utilise the special structure of multi-horizon stochastic programming and propose an enhanced Benders decomposition to solve the model efficiently. We first conduct a sensitivity analysis on retrofitting costs of oil and gas infrastructures. We then compare the REORIENT model with a conventional investment planning model regarding costs and investment decisions. Finally, the computational performance of the algorithm is presented. The results show that: (1) when the retrofitting cost is below 20% of the cost of building new ones, retrofitting is economical for most of the existing pipelines, (2) platform clusters keep producing oil due to the massive profit, and the clusters are abandoned in the last investment stage, (3) compared with a traditional investment planning model, the REORIENT model yields 24% lower investment cost in the North Sea region, and (4) the enhanced Benders algorithm is up to 6.8 times faster than the level set stabilised adaptive Benders decomposition.

Keywords: Stochastic programming, Multi-horizon stochastic programming, Mixed-integer linear programming, Large-scale optimisation, Retrofit of energy systems

---

*Corresponding author

Email addresses: hongyu.zhang@ntnu.no (Hongyu Zhang), grossmann@cmu.edu (Ignacio E. Grossmann), brage.knudsen@sintef.no (Brage Rugstad Knudsen), K.McKinnon@ed.ac.uk (Ken McKinnon), rodrigo.garciana@gmail.com (Rodrigo Garcia Nava), asgeir.tomasgard@ntnu.no (Asgeir Tomasgard)

1. Introduction

Accelerating energy transition in all sectors is vital to achieve a carbon-neutral economy by 2050 (European Commission, 2022, 2020). The committed emissions from existing energy infrastructure jeopardise the 1.5 °C target (Tong et al., 2019). It may be more beneficial to retrofit existing energy infrastructure than to abandon it. Abandoning existing energy infrastructure, such as oil and gas infrastructure, may have a substantial cost (Bakker et al., 2019). Also, the oil and gas industry involves multi-billion-dollar investments and profits. Therefore, there is motivation to retrofit existing oil and gas infrastructure for clean energy production and transportation to (1) help the oil and gas industry transition to a clean energy producer, and (2) accelerate the energy transition by financing it using the gain from the avoided abandonment cost. Retrofitting existing oil and gas infrastructure for hydrogen production and transportation is drawing more attention due to the increasing demand for hydrogen. Most offshore pipelines can be used for hydrogen transport in Europe (Gentile et al., 2021). The European hydrogen infrastructure can grow to a pan-European network by 2040, which is largely based on repurposed existing natural gas infrastructure (Rossum et al., 2022). Retrofitting an existing offshore platform to a green hydrogen production platform is under exploration (Neptune Energy, 2023). We note that retrofitting may become an important pillar for accelerating the energy transition. Therefore, in this paper, we analyse cost drivers that have the possibility to trigger widespread retrofit of offshore oil and gas infrastructure to clean energy generation and decarbonisation purposes. We use a high-fidelity, detailed spatial-temporal stochastic programming model to analyse these drivers for a large region with a substantial role in the energy supply to the surrounding countries.

Energy system infrastructure planning is crucial during the energy transition towards zero emission by 2050. Optimisation models are widely used for the investment (Zhang et al., 2022c; Cho et al., 2022; Munoz & Watson, 2015) and operational (Schulze & McKinnon, 2016; Philpott et al., 2000) planning of energy systems. Traditionally, capacity expansion, retrofitting (Støre et al., 2018) and abandonment are planned separately using different models. However, as sector coupling and Power-to-X become more important, as well as the possibility to retrofit existing infrastructure for renewable energy production and distribution, the ability to analyse investments, retrofit and abandonment planning in a single integrated model becomes more important; including all degrees of freedom together minimises the risk of suboptimality. However, such integrated models have been less explored than their counterparts that treat investment, retrofit and abandonment independently.

Managing uncertainty is crucial in a long-term planning model. Long-term energy system planning problems are normally prone to uncertainty on strategic and operational time horizons. Strategic uncertainty includes oil and gas prices, CO_2 budget, and CO_2 tax. Short-term uncertainty normally includes the availability of non-dispatchable renewable technologies and the failure of conventional generators. Multi-Horizon Stochastic Programming (MHSP) includes uncertainty in both time horizons more efficiently than traditional multi-stage stochastic programming (Kaut et al., 2014). Most previous studies on energy system planning consider only short-term uncertainty

(Backe et al., 2022). In this paper, the proposed model utilises MHSP and includes uncertainty from both time horizons.

The computational difficulty needs to be addressed. The special structure of MHSP allows decomposing of a problem with Benders-type algorithms. A stabilised adaptive Benders decomposition algorithm was proposed in (Zhang et al., 2022a) and demonstrated on a power system investment planning problem with up to 1 billion variables and 4.5 billion constraints. The algorithm showed a significant reduction in computational time. However, Zhang et al. (2022a) dealt with a large-scale linear programming problem. In this paper, we consider a problem with binary variables in the investment planning part in order to capture the economic scale and model retrofit and abandonment decisions. Because the binary variables only exist in the investment planning part, which is the reduced master problem in the Benders-type algorithm, we can still apply stabilised adaptive Benders directly. However, the algorithm may slow down due to the combinatorial part of the problem.

To fill the research gaps mentioned above, we first propose the REORIENT (REnewable resOuRce Investment for the ENergy Transition) model, which is a multi-horizon stochastic Mixed-Integer Linear Programming (MILP) model with short-term and long-term uncertainty for the investment, retrofit and abandonment planning for energy systems. We consider retrofitting existing platforms for offshore green hydrogen production and pipelines for green and blue hydrogen distribution. We then demonstrate the REORIENT model on a European energy system planning problem. An enhanced Benders decomposition is proposed to solve the problem efficiently. we improve the method in (Zhang et al., 2022a) to allow it to solve problems with binary variables faster.

The contributions of the paper are the following: (1) we integrate investment planning, retrofitting, and abandonment in a single stochastic optimisation model, (2) we formulate the problem using multi-horizon stochastic MILP, (3) we propose an enhanced Benders decomposition method to solve such large scale model, and (4) we demonstrate the model on a large-scale planning problem for the European energy system to analyse the planning decisions and costs and provide global insights.

The outline of the paper is as follows: Section 2 introduces the background knowledge regarding capacity expansion planning, retrofit planning and abandonment planning, stochastic programming, MHSP, and Benders decomposition. Section 3 provides the problem description, modelling strategies and assumptions. Section 4 presents the proposed enhanced Benders decomposition. Section 5 presents the REORIENT model. Section 6 reports the computational results and numerical analysis. Section 7 discusses the implications of the method and results and summaries the limitations of the research. Section 8 concludes the paper and suggests further research.

2. Literature review

In the following, we present a brief overview of relevant literature on capacity expansion planning, abandonment planning, retrofit planning, MHSP, and Benders decomposition.

2.1. Capacity expansion planning

Capacity expansion planning problems normally consider an existing system with historical capacity or a new system and make investment planning to fulfil the demand under, among others, environmental restrictions. Capacity expansion problems are formulated either in deterministic models (Lara et al., 2018) or stochastic programming models (Backe et al., 2022; Conejo et al., 2016). Backe et al. (2022) utilised multi-horizon formulation but did not include long-term uncertainty. To capture the economic scale of investment decisions, sometimes MILP is used (Lara et al., 2020). To gain enough environmental and economic insights from such models, sometimes a large-scale problem needs to be modelled, such as (Li et al., 2022; Zhang et al., 2022c). Munoz et al. (2016) proposed a new bounding scheme and combine it with Benders decomposition to solve a large investment planning problem that is formulated as MILP. In addition to planning for power, natural gas and heat systems separately, planning for integrated multi-carrier systems is also studied. Energy hubs that convert, condition and store multiple energy carriers in an investment planning problem were studied in (Zhang et al., 2022a). Stochastic programming is also exploited in natural gas systems (Fodstad et al., 2016), offshore oil and gas infrastructure planning (Gupta & Grossmann, 2014), and hydrogen network (Galan et al., 2019). There is much literature on capacity expansion problems. Therefore, we refer the readers to (Krishnan et al., 2016) for a more comprehensive review.

2.2. Retrofit planning

In grassroots design, the decisions on what processes to use are made first to be followed by equipment decisions, but the retrofit design also requires models that can rate existing equipment for proper analysis. A comparison of grassroots and retrofit design has been presented in (Grossmann et al., 1987). The combinatorial nature of the retrofit planning problems makes such models much more complex. There are several reasons for retrofit, including (1) processing a new feedstock, (2) improving the economics by the use of less energy per unit of production, (3) making a new product, and (4) increasing the conversion of the feedstocks. In this paper, we consider retrofitting to make a new product. A debottlenecking strategy was proposed for retrofit problems (Harsh et al., 1989). A systematic procedure for the retrofit of heat exchanger networks was presented in (Yee & Grossmann, 1991). Retrofit of heat exchangers has been extensively studied in the past decades (Pan et al., 2013; Wang et al., 2012). A high-level optimisation model for the retrofit planning of process networks was presented in (Jackson & Grossmann, 2002), in which the retrofit over several time periods was addressed. The proposed strategy consists of a high-level analysis of the entire network and a low-level analysis of a specific process flowsheet. The problem is formulated using a multi-period generalised disjunctive programming model, which is reformulated using a mixed-integer linear program using the convex hull formulation. In this paper, because of the scope and size of the problem, we only consider the high-level modelling of the retrofit.

2.3. Abandonment planning

Abandonment planning includes the abandonment of power plants that exceed their lifetimes, and of mature oil and gas fields. Existing literature focuses on the plug and abandonment campaign in the oil and gas industry. This is because many wells are planned to be plugged and abandoned, and such activity will have a substantial cost (Bakker et al., 2019). The plug and abandonment cost is estimated at £5-15 million per well, and thousands are expected to be abandoned just in offshore regions over the next decade. Plug and abandonment planning is usually formulated as a profit maximisation problem (Bakker et al., 2021a) or cost minimisation problem (Bakker et al., 2019, 2021b). Real options theory is also used for oil and gas field development (Fleten et al., 2011; Støre et al., 2018; Bakker et al., 2019). In addition to abandonment, investment and operational scheduling optimisation in the oil and gas sector can be found in (Oliveira et al., 2013; Goel & Grossmann, 2004; Gupta & Grossmann, 2012; Iyer et al., 1998).

From the literature above, we find that the planning of investment, retrofit, and plug and abandonment are often treated separately. To overcome the limitations of the separated approach for energy systems planning where such decisions are deemed tightly coupled, we propose a modelling framework that integrates investment, plug and abandonment and retrofit. An illustrative example is presented in Figure 1. The parts marked with red represent the new integrated planning compared with traditional investment planning in the literature.

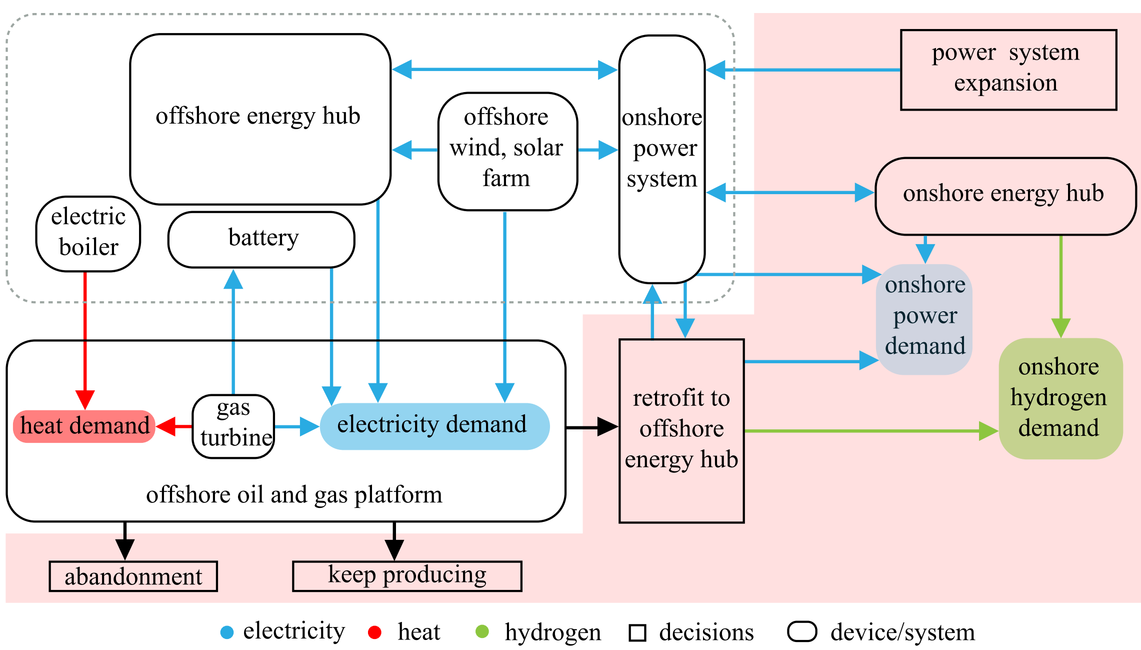

Figure 1: Integrated investment, retrofit and abandonment planning. The grey dotted box includes some technologies that can be invested in. The offshore oil and gas platform can be retrofitted or abandoned. Otherwise, it can keep producing. The Offshore Energy Hubs (OEHs) (Zhang et al., 2022c) can generate electricity, and produce and store hydrogen.

2.4. MHSP

Investment planning of an energy system often faces uncertainty from two time horizons (Kaut et al., 2014; Lara et al., 2020): (a) the uncertainty from the operational time horizon, such as the availability of renewable energies. The operational uncertainty becomes even more crucial

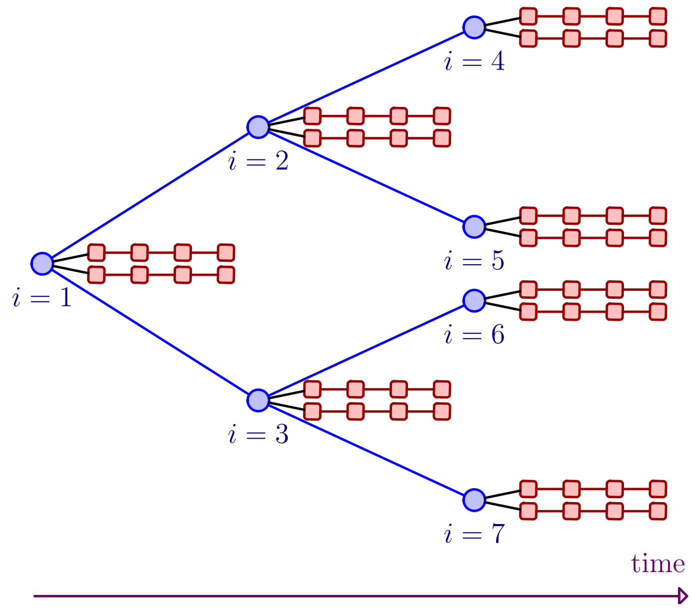

Figure 2: Illustration of MHSP with short-term and long-term uncertainty (blue circles: strategic nodes, red squares: operational periods, i : index of the strategic nodes).

for a system with higher penetration of intermittent renewable energies, and (b) the uncertainty from the strategic time horizon, e.g., oil and gas price and demand. In traditional multi-stage stochastic programming, uncertainty from operational and strategic time horizons can lead to a large scenario tree, thus, an intractable planning model. The multi-horizon approach was proposed as an alternative formulation that reduces the model size significantly (Kaut et al., 2014). An illustration of MHSP with short-term and long-term uncertainty is shown in Figure 2. One can have a much smaller model by disconnecting operational nodes between successive planning stages and embedding them into their respective strategic nodes. We call an operational problem embedded in a strategic node an operational node. The resulting model is called MHSP. MHSP is identical to multi-stage stochastic programming provided two requirements are met (Kaut et al., 2014): (a) strategic and operational uncertainties are independent, and the strategic decisions must not depend on any particular operational decisions, and (b) the operational decisions in the last operational period in a stage do not affect the system operation in the first operational period in the next stage. If either of these conditions is not met then MHSP gives only an approximation. MHSP has been applied in several energy system planning problems (Skar et al., 2016; Backe et al., 2022; Zhang et al., 2022b; Durakovic et al., 2023). Furthermore, the bounds in MHSP have been studied in (Maggioni et al., 2020).

2.5. Benders decomposition

Benders decomposition was proposed to solve problems with complicating variables (Geoffrion & Balakrishnan, 1972). Then generalised Benders for nonconvex problems were proposed (Steeger & Rebennack, 2017; Li & Grossmann, 2019). Extensive research was conducted on accelerating

Benders decomposition, such as by choosing and adding strong cuts (Magnanti & Wong, 1981; Oliveira et al., 2014), developing a multi-cut version of Benders decomposition (You & Grossmann, 2011), regularised Benders decomposition (Zverovich et al., 2012; Zhang et al., 2022a), and using inexact oracles (Mazzi et al., 2020; Zhang et al., 2022a; van Ackooij et al., 2016). In this paper, we adopt the approach from (Zhang et al., 2022a) and improve and extend the method to solve MILPs.

Benders type decomposition algorithms have been used for capacity expansion (Li et al., 2022; Munoz et al., 2016). However, we need another enhanced Benders decomposition for solving the REORIENT model. Standard Benders decomposition was used for solving a two-stage stochastic programming problem (Munoz et al., 2016). In two-stage stochastic capacity expansion problems, the investment decisions are first-stage decision variables, and the operational variables are the recourse variables. However, a capacity expansion problem becomes a multi-stage stochastic program once long-term and short-term uncertainty is included. Nested Benders decomposition is needed to solve a multi-stage stochastic program. However, there is no paper on using nested Benders decomposition to solve a multi-stage stochastic capacity expansion problem with short-term and long-term uncertainty. (Zhang et al., 2022a) first showed that a multi-stage stochastic capacity expansion program formulated as MHSP could be decomposed by standard Benders and proposed the stabilised adaptive Benders decomposition to solve investment planning problems with short-term and long-term uncertainty with up to 1 billion variables and 4.5 billion constraints. As pointed out by (Zhang et al., 2022a), MHSP has a special structure that allows solving multi-stage stochastic programming using standard Benders. Also, when the subproblems differ only in the right-hand side and cost coefficient, Benders decomposition with adaptive oracles can solve MHSP more efficiently. Benders decomposition with adaptive oracles has shown 31.9 times faster than standard Benders decomposition (Mazzi et al., 2020) for a 1% convergence tolerance, and it has been further improved by stabilisation (Zhang et al., 2022a). Therefore, we adopt the stabilised adaptive Benders algorithm in (Zhang et al., 2022a) for solving the REORIENT model. However, the models in (Zhang et al., 2022a; Mazzi et al., 2020) are LPs. The REORIENT model is a mixed-integer MHSP model with short-term and long-term uncertainty and is more complex than the model in (Zhang et al., 2022a). We notice the limitation of the stabilised adaptive Benders when solving the REORIENT model because of the binary variables. Therefore, this paper proposes another enhanced Benders based on (Zhang et al., 2022a) to speed up the stabilisation step.

In addition to Benders decomposition, Lagrangean decomposition (Escudero et al., 2017), column generation (Singh et al., 2009), and combined column generation and Benders decomposition (Huang et al., 2022) have been proposed for capacity expansion problems. However, these approaches did not utilise the special structure of MHSP and are less suitable alternatives than the method in (Zhang et al., 2022a). Although these approaches can solve problems with integer variables in the operational problem, the complexity of the REORIENT model is from the inclusion of short-term and long-term uncertainty rather than integer operational variables. In addition, (Zhang et al., 2022a) first pointed out that stabilisation is very important for the performance of Benders-type decomposition when solving multi-region capacity planning problems, which was not considered in existing Benders type algorithms, such as (Huang et al., 2022; Munoz et al., 2016; Li et al., 2022). Therefore, we choose to use an algorithm that is designed to exploit the special structure of MHSP (Zhang et al., 2022a) and extend the algorithm to solve the REORIENT model.

3. Problem description, modelling strategies, modelling assumptions

In this section, we present the problem description and modelling strategies, including price modelling, scenario generation, temporal and geographical representations of the problem, and the modelling assumptions.

The problem under consideration aims to choose (a) the optimal strategy for investment, abandonment and retrofit planning, and (b) operating scheduling for an energy system to achieve emission targets at minimum overall costs under short-term uncertainty, including renewable energy availability, hydropower production profile and load profile, and long-term uncertainty, including oil and gas prices.

For the investment planning, we consider: (a) thermal generators (Coal-fired plant, OCGT, CCGT, Diesel, nuclear plants, co-firing biomass with 10% lignite, lignite); (b) generators with Carbon Capture and Storage (CCS) (Coal-fired plant with CCS and advanced CCS, gas-fired plant with CCS and advanced CCS, co-firing biomass with 10% lignite with CCS, lignite with CCS, lignite with advanced CCS); (c) renewable generators (onshore and offshore wind and solar, wave, biomass, run-of-the-river hydropower, geothermal and regulated hydropower); (d) electric storage (hydro pump storage and lithium); (e) onshore and offshore transmission lines; (f) onshore and offshore clean energy hubs (electrolyser, fuel cell, hydrogen storage); (g) onshore steam reforming plant with CCS (SMRCCS) and (h) offshore and onshore hydrogen pipelines. The capital costs and fixed operational costs coefficients are assumed to be known.

For the retrofit planning, we consider: (a) retrofitting existing natural gas pipelines for hydrogen transport, and (b) retrofitting existing offshore platforms for clean OEHs. Finally, we consider the abandonment of mature fields. The problem is to determine: (a) the capacities of technologies and retrofit and abandonment decisions, and (b) operational strategies that include scheduling of generators, storage and approximate power flow among regions to meet the energy demand which minimises the combined overall expected investment and operational and environmental costs.

3.1. Modelling strategies and assumptions

In this section, we present the modelling strategies and assumptions we use in the long-term integrated planning problem.

3.1.1. Price process

We use a two-factor Short-Term Long-Term (STLT) model to capture a realistic price behaviour of oil and gas (Schwartz & Smith, 2000). The STLT model has a stochastic equilibrium price and stochastic short-term deviations (Bakker et al., 2021a). In the STLT model, the logarithm of the spot price at time t is,

$$\log p_t = \chi_t + \xi_t, \tag{1}$$

where χ_t is the short-term factor in prices and ξ_t is the long-term factor. (Bakker et al., 2021a) presents a risk-neutral STLT model in discrete time, which is used in this paper for price modelling. The price is represented by,

$$\tilde{p}_t = e^{\tilde{\chi}_t + \tilde{\xi}_t}, \tag{2}$$

$$\tilde{\chi}_t = \tilde{\chi}_{t-1} - \left(1 - e^{-\kappa \Delta t}\right) + \sigma_\chi \epsilon_\chi \sqrt{\frac{1 - e^{-2\kappa\Delta t}}{2\kappa}}, \tag{3}$$

$$\tilde{\xi} = \tilde{\xi}_{t-1} + \mu_\xi^* \Delta t + \sigma_\xi \epsilon_\xi \sqrt{\Delta t}, \tag{4}$$

where $\tilde{p}_t$, $\tilde{\chi}_t$ and $\tilde{\xi}_t$ are risk-neutral equivalents to the spot price, short-term factor and long-term factor. The volatilities are represented by σ_χ and σ_ξ, while ϵ_χ and ϵ_ξ are correlated standard normal random variables with correlation coefficient $\rho_{\chi\xi}$. The parameter κ is the mean reverse coefficient, λ_χ is a risk premium that specifies a reduction in the drift got the short-term process, and μ_ξ^* is the risk-neutral drift of the equilibrium level, $\tilde{\xi}_t$. The length of the time period t (in years) is represented by Δ_t.

Based on the historical record, we assume the gas price is correlated with the oil price, although recently, they have been less correlated due to the energy crisis.

3.1.2. Long-term production profile modelling

There are three phases during the lifetime of oil fields (Støre et al., 2018). We adopt the production modelling from (Wallace et al., 1987). The long-term production profile of oil and gas is presented by,

$$q_t = \begin{cases} q^P & t \le t^P, \\ q^P e^{-m(t-t^p)} & t > t^P, \end{cases} \tag{5}$$

where q^P is the production rate during plateau period, t^P is the length of the plateau period, m is the decline constant. We also calibrate the model with the average decline rate of the giant oil fields in the world (Höök et al., 2009).

3.1.3. Scenario generation

For short-term uncertainty, we consider uncertain time series data including wind and solar capacity factors, hydropower generation profiles, load profiles, and platform production profiles. We consider operational problems with an hourly resolution. We divide the full year into four seasons and select representative time slices from these seasons. The length of the times slices can vary in different seasons. To preserve the auto-correlation and correlation between time series data, the same hours are used for all the time series data within a scenario. The generated operational scenarios are used for all operational nodes.

For long-term uncertainty, we consider oil and gas price uncertainty. We first generate a large number of projections using the price process described in Section 3.1.1. Then we obtain the mean values of the prices for each stage and construct the mean scenario. Next, we use a Julia package

`ScenTrees.jl` (Kirui et al., 2020) that utilises the methodology proposed in (Pflug & Pichler, 2015) to generate a multi-stage scenario tree. Finally, we reduce the scenario tree by removing the decision nodes whose probability is zero.

3.1.4. Geographical representation of the problem

The problem potentially consists of many regions and results in a large model. Therefore, we use a k-means cluster approach to group platform locations into representative locations, adapted from (Zhang et al., 2022c). We use dedicated locations to represent the regions that require higher resolution. All generators and storage units within each aggregated region with the same characteristics are aggregated into clusters. In this way, within aggregated regions, the model does not make the investment in individual units but in the total for that technology.

3.1.5. Modelling assumptions

We assume that: (a) the Kirchhoff voltage law is omitted and we use a linear direct current power flow model for the power system part, (b) the initial storage level of storage units in each operational node are assume to be half of their capacities, (c) the switch from natural gas to hydrogen has little impact on the capacity of a pipeline to transport energy (Fors et al., 2021), (d) linepack in hydrogen pipelines is omitted, (e) investment in new wells is not considered, (f) we simplify the modelling of pressure and temperature of the production processes on platforms and use typical values from the North Sea region, (g) there is no more oil and gas profit once a platform is retrofitted, and the gas profit, associated with a pipeline is lost once it is retrofitted.

4. Benders decomposition in MHSP

MHSP has a structure that allows the application of Benders-type decomposition for solving large-scale stochastic programming problems. In the following, we first present how a MHSP problem can be decomposed by Benders decomposition. We then propose an enhanced Benders decomposition for solving the proposed model efficiently.

4.1. Benders decomposition in MHSP

Here, we give a general formulation for MHSP and show that it has a special structure allowing it to be decomposed by Benders decomposition.

A MHSP model for strategic planning problems can be formulated as follows

$$\min_{x,y} \sum_{i\in\mathcal{I}} \pi_i \left(c_i^\top x_i + \sum_{s\in\mathcal{S}_i} \omega_{is} q_{is}^\top Q_{is} y_{is} \right) \tag{6a}$$

$$\text{s.t. } T_j^I x_j + W_i^I x_i \leq h_i^I, \qquad i \in \mathcal{I}\setminus\{1\}, j = I_i, \tag{6b}$$

$$T^0 x_i \leq h^0, \qquad i = 1, \tag{6c}$$

$$T_{is}^O x_i + W_{is}^O y_{is} \leq h_{is}^O, \qquad i \in \mathcal{I}, s \in \mathcal{S}_i, \tag{6d}$$

where x are the strategic decision variables, $x = \{x_i | i \in \mathcal{I}\}$, and $x_i = \{x_{ij} \in \{0,1\}, j = 1, ..., p; x_{ij} \in \mathbb{R}, j = p+1, ..., n_i\}$ and y are the operational variables, $y = \{y_{is} | i \in \mathcal{I}, s \in \mathcal{S}_i\}$, $y_{is} \in \mathbb{R}^{n_i}$. The π_i is the probability of strategic node i, sum of π_i in each strategic stage is equal to 1, $c_i \in \mathbb{R}^{n_i}$, $h_i^I \in \mathbb{R}^{m_i}$, $W_i^I \in \mathbb{R}^{m_i \times n_i}$, are vectors and matrices at strategic node $i \in \mathcal{I}$, and $T_j^I \in \mathbb{R}^{m_i \times n_j}$ is the matrix for its ancestor node $j = I_i$. The probability of operational scenario s that is embedded in strategic node i is denoted by ω_{is}, and $\sum_{s \in \mathcal{S}_i} \omega_{is} = 1$. Operational vectors and matrices at operational node i, in operational scenario s, are given by $T_{is}^O \in \mathbb{R}^{m_i \times n_i}$, $W_{is}^O \in \mathbb{R}^{m_i \times n_i}$, $q_{is} \in \mathbb{R}^{n_i}$, $h_{is}^O \in \mathbb{R}^{n_i}$.

In MHSP, the complicating variables are the strategic decisions, x_i, that link all the decision nodes. By fixing the complicating variables x_i, we can decompose the full size problem using Benders-type decomposition. For a given node i, the subproblem is formulated as

$$\min_y \pi_i \sum_{s \in \mathcal{S}_i} \omega_{is} q_{is}^\top Q_{is} y_{is} \tag{7a}$$

$$\text{s.t.} \;\; T_{is}^O x_i + W_{is}^O y_{is} \leq h_{is}^O, \qquad i \in \mathcal{I}, s \in \mathcal{S}_i, \tag{7b}$$

the subproblems can be solved in parallel. The reduced master problem is

$$\min_x \sum_{i \in \mathcal{I}} \pi_i (c_i^\top x_i + \beta_i) \tag{8a}$$

$$\text{s.t.} \;\; T_j^I x_j + W_i^I x_i \leq h_i^I, \qquad i \in \mathcal{I} \setminus \{1\}, j = I_i \tag{8b}$$

$$T^0 x_i \leq h^0, \qquad i = 1, \tag{8c}$$

$$\beta_i \geq \theta + \lambda^\top (x_i - x), \qquad (x, \theta, \lambda) \in \mathcal{F}_{i(j-1)}, i \in \mathcal{I}, \tag{8d}$$

where β_i is a variable for the approximated cost of the operational subproblem that is embedded in strategic node i. Constraint (8d) are the Benders cuts built up to iteration $j-1$. To simplify the notation, we write the operational subproblem as

$$g(x_i, c_i) := \min_{y_i \in \mathcal{Y}} \{c_i^\top C y_i | A y_i \leq B x_i\}, \tag{9}$$

where $\mathcal{Y}$ is a convex polyhedron. Also, the Reduced Master Problem (RMP) is,

$$\min_{\mathbf{x} \in \mathcal{X}, \beta} f(\mathbf{x}) + \sum_{i \in \mathcal{I}} \pi_i \beta_i \tag{10a}$$

$$\text{s.t.} \quad \beta_i \geq \theta + \lambda^\top (x_i - x), \qquad (x, \theta, \lambda) \in \mathcal{F}_{i(j-1)}, i \in \mathcal{I}, \tag{10b}$$

where $f(\mathbf{x}) = \sum_{i \in \mathcal{I}} \pi_i c_i x_i$, $\mathcal{X}$ is the feasible region of variable $\mathbf{x}$, $\mathcal{F}_{i(j-1)}$ is the set of cuts associated with subproblem i built up to iteration $j-1$.

4.2. Enhanced Benders decomposition

In this section, we present the solution method for solving the proposed problem. The algorithm is adapted from (Zhang et al., 2022a) and improved for solving MILP. (Zhang et al., 2022a) utilised adaptive oracles (Mazzi et al., 2020) and level method regularisation and achieved a significant reduction in solution time. When $g(x_i, c_i)$ is convex and decreasing w.r.t. x_i, and concave and increasing w.r.t. c_i, one of the adaptive oracles approximates $g(x_i, c_i)$ from below the other from above adaptively. By using these, one can avoid solving all subproblems every iteration to reduce the computational cost compared to standard Benders decomposition. The RMP in adaptive Benders is similar to the one in standard Benders, the set of cuts $\mathcal{F}$ in Equation (10b) different due to the inexact adaptive oracles. The adaptive oracles provide inexact and valid upper and lower bounds on θ, $\overline{\theta}$ and $\underline{\theta}$, and a lower bound on λ, $\underline{\lambda}$. To evaluate adaptive oracles, ϕ, the sensitivity of the cost coefficients from the subproblem is needed. The level set stabilisation problem is to minimise the distance from a previous reference point subject to all the constraints from the RMP and an extra target constraint that is based on the lower and upper bounds and a stabilisation factor, γ that is the ratio of the new targeted bound gap to the existing bound gap. The level set constraint is to restrict the objective value of the RMP. The level method problem is a quadratic program if L_2 norm is used (Zverovich et al., 2012) and becomes a mixed-integer quadratic program after adding integer variables. In this paper, we use a centre point approach to avoid solving the mixed-integer quadratic programming but still obtain a stabilised solution. Finding a well centred point is a built-in function in solvers like Gurobi (Gurobi Optimization, LLC, 2022) with certain solver parameter settings. The solvers utilise some methods to get well centred points. By doing so, the time spent on regularisation is reduced significantly.

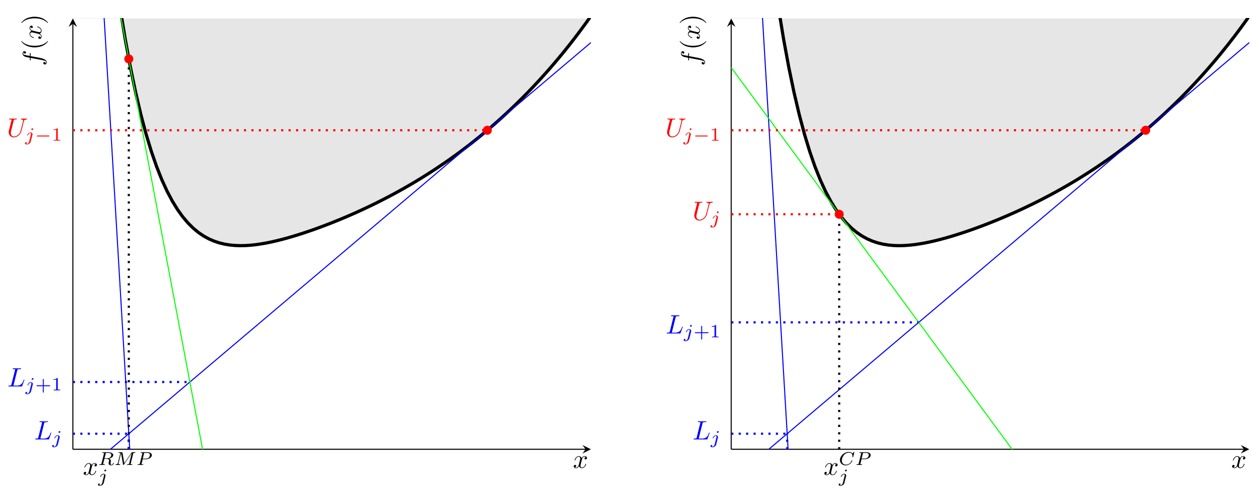

(a) standard Benders

(b) Benders with centre point

Figure 3: An illustrative example of iteration j of standard Benders and Benders with centre point. (Red dots: upper bounds, blue solid lines: cuts built before iteration j, green lines: cuts built in iteration j.)

The Centre Point problem (CP) is the relaxed RMP problem that excludes the objective function and subjects to, in addition to RMP constraints, an extra level set constraint,

$$f(\mathbf{x}) + \sum_{i \in \mathcal{I}} \pi_i \beta_i \leq L_j^* + \gamma (U_{j-1}^* - L_j^*), \tag{11}$$

where U_{j-1}^* and L_j^* are the best upper bound at iteration $j-1$ and lower bound at iteration j, respectively. The CP is a feasibility problem because there is no objective function. An illustration of the centre point approach is presented in Figure 3.

The method is presented in Algorithm 1. The stabilisation factor γ is adjusted using an approach that is analogous to trust region method which is called level set management step. (Zhang et al., 2022a) has pointed out that by adjusting the stabilisation factor, Benders type algorithm is more robust. In the early tests in this paper, we noticed that level set management is much more efficient than using fixed stabilisation factor. We omit the details of the level set management step, and for that refer the readers to (Zhang et al., 2022a).

4.3. Convergence of Algorithm 1

To prove the convergence of Algorithm 1, we first give the following proposition.

Proposition 1. *The Benders cuts generated by calling oracles at $\mathbf{x}^{CP}$ underestimate the objective function value of the original MILP problem.*

Proof. The constraints of CP are linear relaxation of those of the RMP. The $\mathbf{x}^{CP}$ is a feasible solution of CP. It is trivial that the optimal value of the linear relaxation underestimates the optimal value of the original problem. Therefore, following the proof by (Birge, 1985) that Benders cuts are valid for linear programming problems, the Benders cuts are also valid for the original MILP problem. □

Following the convergence proof of Algorithm 2 in (Mazzi et al., 2020) and **Proposition** 1, Algorithm 1 terminates in a finite number of iterations with an ϵ-optimal solution to problem (6).

5. The REORIENT model

This section presents the energy system integrated planning and operational optimisation model. The full model is decomposed by having an investment planning master problem and an operational subproblem. We use the conventions that calligraphic capitalised Roman letters denote sets, upper case Roman and lower case Greek letters denote parameters, and lower case Roman letters denote variables. The indices are subscripts, and name extensions are superscripts. The same lead symbol represents the same type of thing. The names of variables, parameters, sets and indices are single symbols. We give a brief definition of some of the main sets and variables, and their corresponding domains as we explain the equations. For a complete overview of all sets and indices, parameters and variables used in the RIORIENT model, we refer to Appendix A.

5.1. Investment planning model (RMP in Benders decomposition)

The investment master problem Equations (12)-(24) follows the general formulation given by Equations (10). The total discounted cost for investment planning, Equation (12), consists of actual investment costs c^{INV} as well as the expected operational cost of the system over the time horizon $\kappa \sum_{i\in\mathcal{I}^{Ope}} \pi_i c_i^{OPE}$ which is total approximated subproblem costs in Benders decomposition. Here, κ is a scaling factor that depends on the time step between two successive investment nodes. The

Algorithm 1 Regularised Benders decomposition with adaptive oracles

choose ϵ (convergence tolerance), $\gamma \in (0,1)$ (stabilisation factor), $\underline{\beta}$ (initial lower bound β_i), $U_0^* := M$ (initial upper bound), and level set management steps related parameters;
set $j := 0$, $\mathcal{F}_{i0} := \{(\beta_{i0}, 0, 0)\}$ for each $i \in \mathcal{I}$;
solve subproblem at the special point $(\underline{x}, \underline{c})$ and obtain θ, λ and ϕ; set $\mathcal{S} := \{(\underline{x}, \underline{c}, \theta, \lambda, \phi)\}$;
repeat
  set $j := j + 1$;
  solve RMP and obtain β_{ij} and $\mathbf{x}_j^{RMP}$; set $L_j^* := f(\mathbf{x}_j^{RMP}) + \sum_{i \in \mathcal{I}} \pi_i \beta_{ij}$;
  set CP target: $L_j^* + \gamma(U_{j-1}^* - L_j^*)$;
  solve CP and obtain $\mathbf{x}_j^{CP}$;
  for $i \in \mathcal{I}$ **do**
    call adaptive oracles at (x_{ij}^{CP}, c_i) and obtain $\underline{\theta}_{ij}$, $\overline{\theta}_{ij}$, and $\underline{\lambda}_{ij}$;
  end for
  repeat
    $n := n + 1$;
    set $i := \mathrm{argmax}_{i \in \mathcal{I}}\, \pi_i(\overline{\theta}_{ij} - \underline{\theta}_{ij})$;
    solve subproblem i at (x_{ij}^{CP}, c_i) exactly and obtain θ_{ij}, λ_{ij}, ϕ_{ij};
    set $\mathcal{S} := \mathcal{S} \cup \{(x_{ij}^{CP}, c_i, \theta_{ij}, \lambda_{ij}, \phi_{ij})\}$;
    for $i \in \mathcal{I}$ **do**
      call adaptive oracles at (x_{ij}^{CP}, c_i) and obtain $\underline{\theta}_{ij}$, $\overline{\theta}_{ij}$, and $\underline{\lambda}_{ij}$;
    end for
    set $L_j^{LBO} := f(\mathbf{x}_j^{CP}) + \sum_{i \in \mathcal{I}} \pi_i \underline{\theta}_{ij}$;
    set $U_j^{UBO} := f(\mathbf{x}_j^{CP}) + \sum_{i \in \mathcal{I}} \pi_i \overline{\theta}_{ij}$;
  until $U_j^{UBO} - L_j^{LBO} \le U_{j-1}^* - L_{j-1}^*$ **or** $L_j^{LBO} \ge U_{j-1}^*$;
  for $i \in \mathcal{I}$ **do**
    set $\mathcal{F}_{ij} := \mathcal{F}_{i(j-1)} \cup \{(x_{ij}^{CP}, \underline{\theta}_{ij}, \underline{\lambda}_{ij})\}$;
  end for
  for $i \in \mathcal{I}$ **do**
    call adaptive oracles at (x_{ij}^{RMP}, c_i) and obtain $\underline{\theta}_{ij}$, $\overline{\theta}_{ij}$, $\overline{\phi}_{ij}$ and $\underline{\lambda}_{ij}$;
  end for
  set $U_j := f(\mathbf{x}_j^{RMP}) + \sum_{i \in \mathcal{I}} \pi_i \overline{\theta}_{ij}$;
  set $U_j^* := \min(U_{j-1}^*, U_j)$;
  level set management steps;
until $U_j^* - L_j^* \le \epsilon$.

scaling factor scales the operational costs between two successive investment nodes. By doing this, we can evaluate the operational subproblem on the represented operational hours and scale the cost up to obtain the total operational costs. Equation (13) calculates the investment cost which comprises capacity-dependent and capacity-independent costs, retrofitting costs, abandonment costs, fixed operating and maintenance costs, and profit of existing technology (e.g., oil and gas platform).

$$\min c^{INV} + \kappa \sum_{i \in \mathcal{I}^{Ope}} \pi_i c_i^{OPE}, \tag{12}$$

where

$$c^{INV} = \sum_{i\in\mathcal{I}^{Inv}} \pi_i^{Inv} \left(\sum_{p\in\mathcal{P}} \left(C_{pi}^{InvV} x_{pi}^{Inv} + C_{pi}^{InvF} y_{pi}^{Inv} \right) + \sum_{p\in\mathcal{P}^{RT}} \left(C_{pi}^{ReTV} x_{pi}^{ReT} + C_{pi}^{ReTF} y_{pi}^{ReT} \right) \right) + \kappa \sum_{i\in\mathcal{I}^{Ope}} \pi_i^{Ope} \left(\sum_{p\in\mathcal{P}} C_{pi}^{Fix} x_{pi}^{Acc} + \sum_{p\in\mathcal{P}^{RT}} C_{pi}^{ReTFixO} x_{pi}^{AccReT} + \sum_{p\in\mathcal{P}^{R}} C_{pi}^{ReFFixO} x_{pi}^{AccReF} \right). \tag{13}$$

Constraint (14) states that the accumulated capacity of a technology x_{pi}^{Acc} in an operational node equals the sum of the historical capacity X_p^{Hist} and newly invested capacities x_{pi}^{Inv} in its ancestor investment nodes $\mathcal{I}_i^{Inv}$ that are not retired.

$$x_{pi}^{Acc} = X_{pi}^{Hist} + \sum_{j\in\mathcal{I}_i^{Inv}|\kappa(S_i^{Ope}-S_j^{Inv})\leq H_p} x_{pj}^{Inv}, \qquad p\in\mathcal{P}, i\in\mathcal{I}^{Ope}. \tag{14}$$

Constraint (15) ensures the maximum X_{pi}^{MaxInv} capacity that is built in an investment node. The binary variable y_{pi}^{Inv} equals 1 if a technology $p\in\mathcal{P}$ in investment node $i\in\mathcal{I}^{Inv}$ is invested. Parameter X_p^{MaxAcc} gives the maximum capacity that can be installed for different technologies.

$$x_{pi}^{Inv} \leq X_{pi}^{MaxInv} y_{pi}^{Inv}, \qquad p\in\mathcal{P}, i\in\mathcal{I}^{Inv}. \tag{15}$$

Constraints (16)-(18) establish that the invested capacity and accumulated capacity of newly invested technologies and retrofitted technologies should be within the capacity limits.

$$x_{pi}^{Acc} \leq X_p^{MaxAcc}, \qquad p\in\mathcal{P}, i\in\mathcal{I}^{Ope}, \tag{16}$$

$$x_{pi}^{AccReT} \leq X_p^{MaxAccReT}, \qquad p\in\mathcal{P}^{RT}, i\in\mathcal{I}^{Ope}, \tag{17}$$

$$x_{pj}^{ReT} \leq X_p^{MaxReT} y_{pi}^{ReT}, \qquad p\in\mathcal{P}^{RT}, i\in\mathcal{I}^{Inv}, j\in\mathcal{I}_i^{Inv}. \tag{18}$$

Constraint (19) dictates that the existing capacity is zero if a technology is retrofitted to a new technology.

$$x_{pj}^{AccReF} = X_{pj}^{HistReF}(1-y_{pi}^{ReF}), \qquad p\in\mathcal{P}^{R}, i\in\mathcal{I}^{Inv}, j\in\mathcal{I}_i^{Ope}. \tag{19}$$

Constraint (20) states that only one technology can be retrofitted to.

$$\sum_{p\in\mathcal{P}_p^R} y_{pi}^{ReT} \leq y_{pi}^{ReF}, \qquad p\in\mathcal{P}^{R}, i\in\mathcal{I}^{Inv}. \tag{20}$$

Constraint (21) ensures that retrofit can only happen once for a technology during the planning horizon.

$$\sum_{i\in\mathcal{I}^{Inv}} y_{pi}^{ReF} \leq 1, \qquad p\in\mathcal{P}^{R}. \tag{21}$$

Constraint (22) states that the accumulated capacity of a technology x_{pi}^{AccReT} in an operational node equals the newly invested capacities x_{pi}^{ReT} in its ancestor investment nodes $\mathcal{I}_i^{Inv}$ that are not retired. Parameter $X_p^{MaxAccReT}$ is the maximum accumulated capacity of a technology that is retrofitted from another.

$$x_{pi}^{AccReT} = \sum_{j\in\mathcal{I}_i^{Inv}|\kappa(S_i^{Ope}-S_j^{Inv})\leq H_p} x_{pj}^{ReT}, \qquad p\in\mathcal{P}^{RT}, i\in\mathcal{I}^{Ope}. \tag{22}$$

The Benders cuts built up to iteration $k-1$ are given by Equation (23).

$$c_i^{OPE} \geq \theta + \lambda^\top(x_i - x), \qquad (x,\theta,\lambda)\in\mathcal{F}_{i(k-1)}, i\in\mathcal{I}. \tag{23}$$

The domains of variables are given as follows

$$x_{pi}^{Inv}, x_{pi}^{Acc}, x_{pi}^{ReT}, x_{pi}^{AccReT}, x_{pi}^{AccReF}, c^{INV} \in \mathbb{R}_0^+, \qquad y_{pi}^{Inv}, y_{pi}^{ReF}, y_{pi}^{ReT} \in \{0,1\}. \tag{24}$$

The vector $x_i = \left(\{x_{pi}^{Acc}, p\in\mathcal{P}\}, \{x_{pi}^{AccReT}, p\in\mathcal{P}^{RT}\}, \{x_{pi}^{AccReF}, p\in\mathcal{P}^{R}\}, \mu_i^{DP}, \mu_i^{DH}, \mu_i^{DHy}, \mu_i^{E}\right)$ collects all right-hand side coefficients that will be fixed in operational subproblem, Equations (25)-(37). The vector $c_i = \left(C_i^{CO_2}\right)$ collects all the cost coefficients. The vectors x_i and c_i will be fixed as parameters in the operational problem. The long-term uncertain parameters including load scaling μ_i^{DP}, μ_i^{DH}, and μ_i^{DHy} μ_i^{E} are fixed in the following operational problem because they affect the system operation.

5.2. Operational problem (subproblem in Benders decomposition)

We now present the operational problem and note that we omit index i in the operational model for ease of notation because all variables and parameters are defined for each operational node.

The right hand side parameters P_p^{Acc}, V_c^{Acc}, P_g^{AccG}, $P_g^{AccHRor}$, P^{AccSE}, Q_s^{AccSE}, P_l^{AccL}, V_l^{AccLHy}, μ^{DP}, μ^{DH}, μ^{E} , μ^{DHy} are fixed by the solution x_i from solving the master problem Equations (12)-(24). The CO_2 cost of generators that is included in parameter C_g^G is fixed by c_i from the master problem.

The operational cost $c^{OPE}(x_i, c_i)$ at one operational node i is computed by solving subproblem Equations (25)-(37) given the decisions x_i and c_i made in Equations (12)-(23). The operational subproblem Equations (25)-(37) correspond to the general formulation Equations (9). The objective function, the operational cost, includes total operating costs of generators $C_g^G p_{gt}^G$, energy load shedding costs for heat, power, and hydrogen $C^{Shed}p_{zt}^{Shed}$ and $C^{Shed}v_{zt}^{Shed}$ and fuel cost of steam reforming plants $C^R v_{rt}^R$. C_g^G includes the variable operational cost, fuel cost and the CO_2 tax, C^{CO_2}, charged on the emissions of generator g. The inclusion of load shedding variables p_{zt}^{Shed} and v^{ShedHy} ensures the operational problem is always feasible. The load shedding costs C^{Shed} are high enough so that the optimal solution has little or nor load shed.

$$\min \sum_{t\in\mathcal{T}} \pi_t H_t \left(\sum_{g\in\mathcal{G}} C_g^G p_{gt}^G + \sum_{r\in\mathcal{R}} C^R v_{rt}^R + \sum_{z\in\mathcal{Z}} \left(\sum_{l\in\{H,P\}} C^{Shed,l} p_{zt}^{Shed,l} + C^{ShedHy} v_{zt}^{ShedHy} \right)\right). \tag{25}$$

Constraints (26) ensure that the technologies operate within their capacity limits.

$$
\begin{aligned}
& p_{pt} \le P_p^{Acc}, && p \in \mathcal{P}^*, t \in \mathcal{T}, && \text{(26a)}\\
& v_{vt} \le V_v^{Acc}, && v \in \mathcal{V}^*, t \in \mathcal{T}, && \text{(26b)}\\
& p_{gt}^{G} + p_{gt}^{ResG} \le P_g^{AccG}, && g \in \mathcal{G}, t \in \mathcal{T}, && \text{(26c)}\\
& p_{st}^{SE-} + p_{st}^{ResSE} \le P_s^{AccSE}, && s \in \mathcal{S}^E, t \in \mathcal{T}, && \text{(26d)}\\
& q_{st}^{SE} \le Q_s^{AccSE}, && s \in \mathcal{S}^E, t \in \mathcal{T}, && \text{(26e)}\\
& -P_l^{AccL} \le p_{lt}^{L} \le P_l^{AccL}, && l \in \mathcal{L}, t \in \mathcal{T}, && \text{(26f)}\\
& -V_l^{AccLHy} \le v_{lt}^{LHy} \le V_l^{AccLHy}, && l \in \mathcal{L}^{Hy}, t \in \mathcal{T}. && \text{(26g)}
\end{aligned}
$$

Constraint (27) captures how fast generators can ramp up or ramp down their power output, respectively.

$$
-\alpha_g^G P_g^{AccG} \le p_{gt}^{G} + p_{gt}^{ResG} - p_{g(t-1)}^{G} - p_{g(t-1)}^{ResG} \le \alpha_g^G P_g^{AccG}, \qquad g \in \mathcal{G}, n \in \mathcal{N}, t \in \mathcal{T}_n. \tag{27}
$$

Constraint (28) dictates that the spinning reserve of generator p_{gt}^{ResG}, plus the reserve of the electricity storage p_{st}^{ResES} must exceed the minimum reserve requirement, where σ^{Res} is a percentage of the power load.

$$
\sum_{g \in \mathcal{G}_z} p_{gt}^{ResG} + \sum_{s \in \mathcal{S}_z^E} p_{st}^{ResSE} \ge \sigma_z^{Res} P_{zt}^{DP}, \qquad z \in \mathcal{Z}, t \in \mathcal{T}. \tag{28}
$$

Constraints (29) and (30) ensure that run-of-the-river hydropower and regulated hydropower production are within their limits and according to the generation profiles, separately.

$$
\sum_{t \in \mathcal{T}_n} p_{gt}^{H} \le \sum_{t \in \mathcal{T}_n} P_{gt}^{HSea}, \qquad g \in \mathcal{G}^{HSea}, n \in \mathcal{N}, \tag{29}
$$

$$
p_{gt}^{H} \le P_{gt}^{HRor} P_g^{AccHRor}, \qquad g \in \mathcal{G}^{HRor}, t \in \mathcal{T}. \tag{30}
$$

Constraint (31) ensures that, in one operational period t, the sum of total power generation of generators p_{gt}^{G}, power discharged from all the electricity storage p_{st}^{SE-}, renewable generation $R_{zt}^{R} p_{rt}^{AccR}$, hydro power generation p_{gt}^{H}, fuel cell generation p_{ft}^{F}, power transmitted to this region, and load shed p_{zt}^{ShedP} equals the sum of power demand $\mu^{DP} P_{zt}^{DP}$, power consumption of electric boilers p_{bt}^{BE}, power consumption of all electrolysers p_{et}^{E}, power transmitted to other regions, and power generation shed p_{zt}^{GShedP}. The parameter R_{rt}^{GR} is the capacity factor of the renewable unit that is a fraction of the nameplate capacity P^{AccR}. The subset of a technology in the region z is represented by $R_z := \{r \in \mathcal{R} : r \text{ is available in region } z\}$, where $\mathcal{R}$ can be replaced by other sets of technologies. The power load shed p^{ShedP} allows power demand unmet at a high cost to ensure feasibility of the operational subproblem. The same idea applies to hydrogen mass balance and heat energy balance.

$$\sum_{g\in\mathcal{G}_z} p^G_{gt} + \sum_{l\in\mathcal{L}^{In}_z} \eta^L p^L_{lt} + \sum_{s\in\mathcal{S}^E_z} p^{SE-}_{st} + \sum_{r\in\mathcal{G}^R_z} R^{GR}_{rt} P^{AccGR}_r + \sum_{g\in\mathcal{G}^H_z} p^H_{gt} + \sum_{f\in\mathcal{F}_z} p^F_{ft} + p^{ShedP}_{zt} =$$
$$\mu^{DP} P^{DP}_{zt} + \sum_{b\in\mathcal{B}^E_z} p^{BE}_{bt} + \sum_{e\in\mathcal{E}_z} p^E_{et} + \sum_{l\in\mathcal{L}^{Out}_z} \eta^L_l p^L_{lt} + \sum_{s\in\mathcal{S}^E_z} p^{SE+}_{st} + p^{GShedP}_{zt}, \qquad z\in\mathcal{Z}, t\in\mathcal{T}. \tag{31}$$

The hydrogen mass balance Constraint (32) dictates that hydrogen produced by electrolyser $H_t\rho^E p^E_{et}$ and steam reforming plant v^R_{rt}, hydrogen transmitted to this region, withdraw from a hydrogen storage v^{SHy-}_{st} and hydrogen production shed $v^{GShedHy}_{zt}$ equals the hydrogen demand V^{DHy}_{zt}, fuel supply to fuel cell $H_t\rho^F p^F_{ft}$, hydrogen injected into the storage v^{SHy+}, hydrogen transmitted from this region plus the hydrogen load shed v^{ShedHy}_{zt}.

$$\sum_{s\in\mathcal{S}^{Hy}_z} v^{SHy+}_{st} + \sum_{l\in\mathcal{L}^{HyOut}_z} v^{LHy}_{lt} + \sum_{f\in\mathcal{F}_z} H_t\rho^F p^F_{ft} + v^{ShedHy}_{zt} + \mu^{DHy} V^{DHy}_{zt} =$$
$$\sum_{l\in\mathcal{L}^{HyIn}_z} v^{LHy}_{lt} + \sum_{e\in\mathcal{E}_z} H_t\rho^E p^E_{et} + \sum_{r\in\mathcal{R}_z} v^R_{rt} + \sum_{s\in\mathcal{S}^{Hy}_z} v^{SHy-} + v^{GShedHy}_{zt}, \qquad z\in\mathcal{Z}, t\in\mathcal{T}. \tag{32}$$

The heat energy balance Constraint (33) states that the heat recovery of gas turbines $\eta^{HrG}_g p^G_{gt}$, plus electric boiler heat generation $\eta^{BE}_b p^{BE}_{bt}$, plus heat load shed p^{ShedH}_{zt} equals the heat demand $\mu^{DH} P^{DH}_{zt}$ plus the heat generation shed p^{GShedH}_{zt}.

$$\sum_{g\in\mathcal{G}} \eta^{HrG}_g p^G_{gt} + \sum_{b\in\mathcal{B}^E_z} \eta^{BE}_b p^{BE}_{bt} + p^{ShedH}_{zt} = \mu^{DH} P^{DH}_{zt} + p^{GShedH}_{zt}, \qquad z\in\mathcal{Z}^P, t\in\mathcal{T}. \tag{33}$$

Constraint (34) states that the state of charge q^{SE}_{st} in period $t+1$ depends on the previous state of charge q^{SE}_{st}, the charged power $\mu^{SE}_s p^{SE+}_{st}$ and discharged power p^{SE-}_{st}. The parameter η^{SE}_s represent the charging efficiency.

$$q^{SE}_{s(t+1)} = q^{SE}_{st} + H_t(\eta^{SE}_s p^{SE+}_{st} - p^{SE-}_{st}), \qquad s\in\mathcal{S}^E, n\in\mathcal{N}, t\in\mathcal{T}_n. \tag{34}$$

The hydrogen storage balance Constraint (35) shows that the hydrogen storage level v^{SHy}_{st} at period $t+1$ equals to storage level at the previous period, plus the hydrogen injected v^{SHy+}_{st}, minus the hydrogen withdrawn v^{SHy-}_{st}.

$$v^{SHy}_{s(t+1)} = v^{SHy}_{st} + v^{SHy+}_{st} - v^{SHy-}_{st}, \qquad s\in\mathcal{S}^{Hy}, n\in\mathcal{N}, t\in\mathcal{T}_n. \tag{35}$$

Constraint (36) restricts the total emission. The parameter μ^E is the CO_2 budget.

$$\sum_{t\in\mathcal{T}} \pi_t \left(\sum_{g\in\mathcal{G}} E^G_g p^G_{gt} + \sum_{r\in\mathcal{R}} E^R v^R_{rt} \right) \le \mu^E. \tag{36}$$

The domains of variables are given as follows

$$\begin{aligned}p_{lt}^{L}, v_{lt}^{LHy} \in \mathbb{R}, \quad p_{gt}^{G}, p^{ShedP}, p^{ShedH}, v_{zt}^{ShedHy}, p_{p}^{Acc}, p_{bt}^{BE}, p^{ResG}, p^{ResSE} \in \mathbb{R}_0^+, \\ p_{g}^{AccG}, p_{zt}^{GShedP}, p_{zt}^{GShedH}, v_{zt}^{GShedHy}, v_{st}^{SHy+}, v_{st}^{SHy-}, v_{st}^{SHy}, p_{et}^{E}, p_{gt}^{H}, p_{r}^{AccGR} \in \mathbb{R}_0^+, \\ p_{st}^{SE+}, v_{l}^{AccLHy}, p_{st}^{SE-}, q_{s}^{AccSE}, q_{st}^{SE}, p_{l}^{AccL}, p_{r}^{AccR}, p_{ft}^{F}, v_{rt}^{R} \in \mathbb{R}_0^+.\end{aligned} \tag{37}$$

6. Results

In this section, we first present the case study. Then we report the computational performance of the enhanced Benders decomposition, followed by the sensitivity analysis of the retrofitting cost of natural gas pipelines and offshore platforms. Finally, we compare the solutions and costs between the REORIENT and investment-only models. The investment-only model is the REORIENT model without the retrofit and abandonment planning functions.

6.1. Case study

We demonstrate the REORIENT model on the integrated strategic planning of the European energy system. The network topology is shown in Figure 4. We make investment planning towards

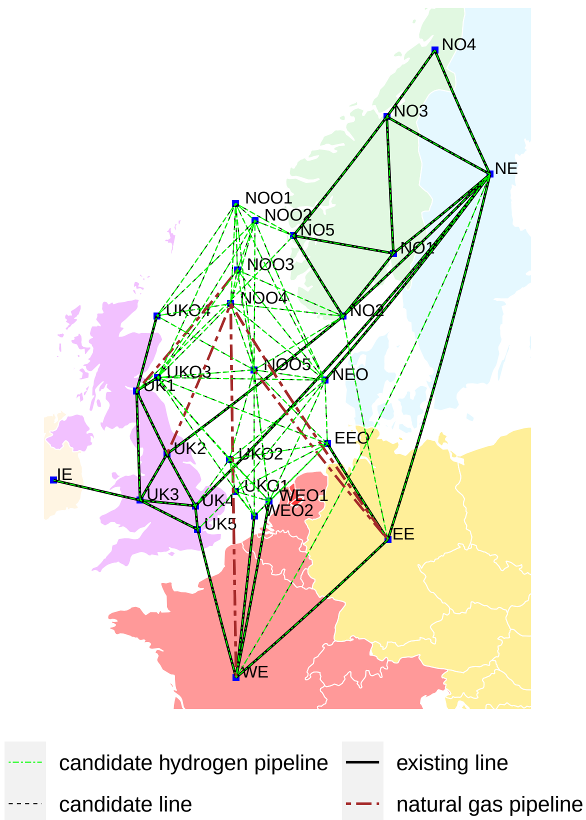

Figure 4: Illustration of the considered European energy system. The considered system includes 27 regions (each region can deploy 36 technologies), 87 transmission lines, 7 existing natural gas pipelines that can be retrofitted for hydrogen transport (some are overlapped), and 87 candidate new hydrogen pipelines.

2050 with a 5-year planning step. We implemented the algorithm and model in Julia 1.8.2 using

JuMP (Dunning et al., 2017) and solved with Gurobi 10.0 (Gurobi Optimization, LLC, 2022). The problem instances contain up to 13 million continuous variables, 1860 binary variables, and 30 million constraints. We run the code on nodes of a computer cluster with a 2x 3.6GHz 8 core Intel Xeon Gold 6244 CPU and 384 GB of RAM, running on CentOS Linux 7.9.2009. The parameters for the price process for oil and gas prices are presented in Table 1.

Table 1: Estimated parameters for the price process, taken from (Bakker et al., 2021a).

	κ	σ_χ	λ_χ	σ_ξ	μ_ξ^*	$\rho_{\chi\xi}$
Estimate	0.407	0.273	-0.147	0.149	-0.007	0.306

Table 2: Existing natural gas pipelines considered in the case study and their potential hydrogen transport capacity.

Model name	Name	From	To	Capacity (Ktonne/hour)
Pipeline 1	Vesterled	NOO3	UK1	0.46
Pipeline 2	Langeled	NOO4	UK2	0.98
Pipeline 3	Zeepipe 1	NOO4	WE	0.58
Pipeline 4	Franpipe	NOO4	WE	0.75
Pipeline 5	Norpipe	NOO5	EE	0.61
Pipeline 6	Europipe 1	NOO4	EE	0.69
Pipeline 7	Europipe 2	NOO4	EE	0.92

We use Gurobi as the base solver. We use the dual simplex algorithm to solve the RMP due to its relatively small size. The parameter `DegenMoves` has been turned on because we notice degeneracy makes the solver slow. We use the Barrier algorithm to solve the centre point problem to obtain a centre point. If `Presolve` is off and `Crossover` is off, then Gurobi will give a centre point. However, we turn on `Presolve` to reduce the problem size further. In addition, considering the scale of the problem, we choose to solve all the following instances to 1% convergence tolerance.

6.1.1. *Computational results*

This section presents an overview of the problem instances and a performance analysis of the proposed algorithm. An overview of the test instances is presented in Table 3. In the test instances, we consider operational problems with hourly time resolution. The test instances vary in the number of operational hours in each short-term scenario, short-term scenarios, and long-term scenarios. The problem instances have six stages, which makes the problem instances big even with a few realisations of the parameters in each stage. The computational time is given in Tables 4 and 5, and note that Gurobi cannot solve Cases 2 and 3.

Table 3: Overview of the cases used in the computational study.

	Operational periods	Short-term	Long-term	Number of decision nodes		Problem size (undecomposed)		
	per short-term scenario	scenarios	scenarios	Operational nodes	Investment nodes	Continuous variables	Binary variables	Constraints
Case 1	96	4	1	6	6	7.0×10^5	180	1.6×10^6
Case 2	672	4	1	6	6	4.8×10^6	180	1.1×10^7
Case 3	96	4	53	114	62	1.3×10^7	1860	3.0×10^7
Case 4	672	8	53	114	62		1860	
Case 5	96	4						
Case 6	672	8						

Table 4: Computational time of level set stabilised Benders. (Iters: iterations, Evals: subproblem evaluations)

	Iters/Evals	Total time spent (h)	Master problem (%)	Stabilisation problem (%)	Subproblems and adaptive oracles (%)	Lower bound	Upper bound
Case 1	714/3615	5.53	16.34	43.06	40.58		
Case 2	894/4249	31.04	4.02	12.76	83.21		
Case 3							
Case 4							
Case 5							
Case 6							

This method did not solve Case 3 after 10 days of running, and it reached 34.6% convergence tolerance before termination.

Table 5: Computational time of centre point stabilised Benders. (Iters: iterations, Evals: subproblem evaluations)

	Iters/Evals	Total time spent (h)	Master problem (%)	Stabilisation problem (%)	Subproblems and adaptive oracles (%)	Lower bound (	Upper bound
Case 1	152/641	0.37	8.42	3.35	88.08		
Case 2	119/516	4.54	0.44	0.20	99.35		
Case 3	161/6502	49.61	9.26	8.88	81.85		
Case 4							
Case 5							
Case 6							

By comparing Tables 4 and 5, we can see that by utilising the centre point, we reduce the computational time significantly. By comparing the percentage of the time spent on solving the stabilisation problem, we can see that solving CP takes much less of the total time than solving a quadratic programming stabilisation problem. We can also see that as we increase the number of strategic nodes, the percentage of time spent on the RMP and CP increases in both algorithms. This is because we add one cut per node per iteration, and as we have more nodes, the RMP and CP grow faster every iteration. Also, by comparing Cases 2 and 3, we observe no significant difference in the number of iterations, but the increase in time is more significant. This is because Cases 2 and 3 have the same amount of strategic decisions, but the subproblem in Case 3 is larger.

6.1.2. Sensitivity analysis

In this section, we use Case 3 to conduct a sensitivity analysis on the fixed retrofitting cost of pipelines and platforms. In addition, we also present the results of the investment decisions for a future energy system with a large amount of green and blue hydrogen production and transportation.

We first conduct a sensitivity analysis on the retrofitting cost of natural gas pipelines. To this end, we consider two cases: Case A, oil and gas production has stopped, and there is no natural gas transportation value in the pipelines, and Case B, oil and gas production is ongoing, and the natural gas pipelines are used for natural gas transport. Using Case A, our motivation is to understand under what cost range it would be more beneficial to retrofit natural gas pipelines that are not in operation compared with building new hydrogen pipelines. Case B is a more realistic case because most of the pipelines in the North Sea are in operation and have an export role. Using Case B, we want to analyse if retrofit to hydrogen will occur if that means the loss of oil and gas export profit. According to Fors et al. (2021), the cost of retrofitting the pipelines can be estimated at around 10-15% of the new construction. Here, we conduct sensitivity on the cost from 5%-30% with a 5% step.

From Table 6, for pipelines 2-7, if the retrofitting cost is below 15% of newly built cost, they will be retrofitted in all scenarios. However, for pipeline 1, when the retrofitting cost is less than 15% of building a new one, it is retrofitted in 28 scenarios, and the retrofitting takes place in the third strategic stage. Pipeline 5 is only retrofitted at the end of the planning horizon when the cost is 15% of building a new one. When the retrofitting cost is higher than 20%, some of the pipelines are not retrofitted. Instead, the model decides to build new pipelines and a different network topology to achieve the minimum cost. We can see that different oil and gas price scenarios affect the retrofitting decisions.

Table 6: Results of the expected retrofitting decisions in Case A.

Cost (% of new one)	Pipeline 1	Pipeline 2	Pipeline 3	Pipeline 4	Pipeline 5	Pipeline 6	Pipeline 7
5%	(0, 0, 2, 4, 8, 16, 28)	$*$	$*$	$*$	$*$	$*$	$*$
10%	(0, 0, 2, 4, 8, 16, 28)	$*$	$*$	$*$	$*$	$*$	$*$
15%	(0, 0, 2, 4, 8, 16, 28)	$*$	$*$	$*$	(0, 0, 0, 0, 0, 2, 3)	$*$	$*$
20%	$-$	$*$	$*$	$-$	$-$	$*$	$*$
25%	$-$	$-$	$*$	$*$	(0, 0, 0, 2, 4, 7, 11)	$*$	$*$
30%	$-$	$-$	$*$	$-$	(0, 0, 0, 0, 2, 4, 7)	$*$	$*$

$*$: the pipeline is retrofitted in all strategic nodes, $-$: the pipeline is not retrofitted.
$(\{x_i, i = 1, .., 7\})$: the number of decision nodes, x_i, that retrofitting of the pipeline takes place in stage i.

Table 7: Results of the expected retrofitting decisions in Case B.

Cost (% of new one)	Pipeline 1	Pipeline 2	Pipeline 3	Pipeline 4	Pipeline 5	Pipeline 6	Pipeline 7
5%	$-$	(0, 0, 0, 0, 2, 4, 6)	(0, 0, 0, 2, 4, 8, 14)	(0, 0, 0, 0, 2, 4, 7)	(0, 0, 0, 0, 2, 4, 8)	(0, 0, 0, 0, 2, 4, 7)	(0, 0, 0, 0, 2, 4, 7)
10%	$-$	$-$	(0, 0, 0, 2, 4, 8, 14)	(0, 0, 2, 4, 8, 16, 28)	(0, 0, 0, 0, 0, 2, 4)	(0, 0, 0, 2, 4, 8, 14)	(0, 0, 0, 2, 4, 8, 14)
15%	$-$	$-$	(0, 0, 0, 2, 4, 8, 14)	(0, 0, 0, 2, 4, 8, 14)	(0, 0, 0, 0, 2, 4, 6)	(0, 0, 0, 2, 4, 8, 14)	(0, 0, 0, 0, 2, 4, 7)
20%	$-$	$-$	(0 ,0, 0, 0, 2, 4, 8)	(0, 0, 0, 0, 2, 4, 6)	(0, 0, 0, 0, 2, 4, 6)	(0, 0, 0, 0, 2, 4, 8)	(0, 0, 0, 0, 2, 4, 8)
25%	$-$	$-$	(0, 0, 0, 2, 4, 8, 14)	(0, 0, 0, 0, 2, 4, 6)	(0, 0, 0, 0, 2, 4, 6)	(0, 0, 0, 2, 4, 8, 14)	(0, 0, 0, 2, 4, 8, 14)
30%	$-$	$-$	$-$	$-$	$-$	(0, 0, 0, 0, 2, 4, 8)	(0, 0, 0, 0, 2, 4, 6)

$-$: the pipeline is not retrofitted.
$(\{x_i, i = 1, .., 7\})$: the number of decision nodes, x_i, that retrofitting of the pipeline takes place in stage i.

From Table 7, it can be observed, compared with Case A, that the economic viability of pipeline retrofit is harder if the pipelines are already used for natural gas transport. However, most pipelines are still retrofitted for hydrogen transportation in later investment stages. From Tables 6 and 7, we can see that retrofit decisions are sensitive to the retrofitting cost, and oil and gas prices. Also, retrofit sometimes only take place in specific price scenarios.

Secondly, we conduct a sensitivity analysis on the retrofitting cost of oil and gas platforms. By doing so, we aim to analyse: (1) if retrofitting can help delay or even avoid the costly abandonment campaign and (2) understand the relation between retrofitting existing platforms for OEHs and building new OEHs. We assume that the fixed part of the retrofitting cost is half of the removal cost, and conduct sensitivity around this cost. For each platform cluster, we consider a fixed part of the retrofitting cost ranging from €10 million to €2 billion. However, the results suggest that it is not economical to retrofit platforms for hydrogen production under this price range due to the massive loss of oil and gas export profit. The model decides to conduct an abandonment campaign for all platform clusters by the end of the planning horizon. This means that based on the cost models that are used, retrofitting platforms for hydrogen production is more costly than abandonment. Also, due to the oil and gas export profit, the platforms will produce as long as possible until they must be abandoned. In this case study, the platforms must be retrofitted or abandoned by 2050. This suggests that repurposing platforms for other use may need stronger incentives in addition to economic factors.

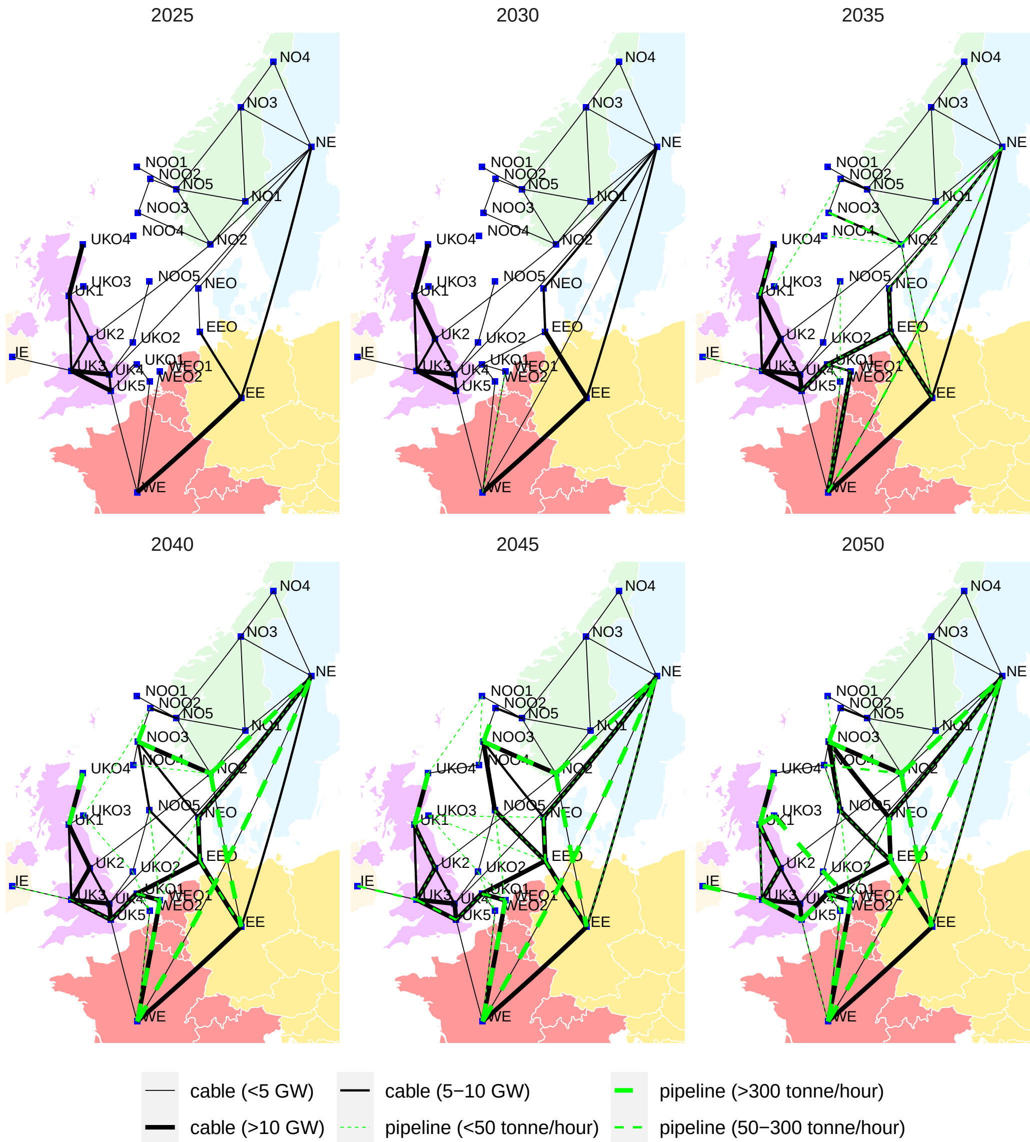

Figure 5: Expected solution of the grid design towards 2050 (investment only model).

6.1.3. Comparison between the REORIENT model and an investment planning only model

In this section, we use Case 3 and analyse the difference between an investment-planning-only model and the proposed integrated model regarding investment decisions and costs. We fix the retrofitting cost of pipelines to 15% of the cost of its newly built counterpart. In the following, we report the results of expected strategic decisions regarding the grid design and capacities of the technologies in each decision stage.

From Figures 5 and 6, we can see that the network topology is noticeably different. By 2050, there will be 32 pipelines built compared with 28 pipelines in the investment-only model. The line connecting NE and NO1 has less capacity in the REORIENT model compared with the investment-only model. In both cases, the UK onshore power system transmission is reinforced, however, a 3 GW difference in the line connecting UK3 and UK5 is observed, followed by a 2 GW difference

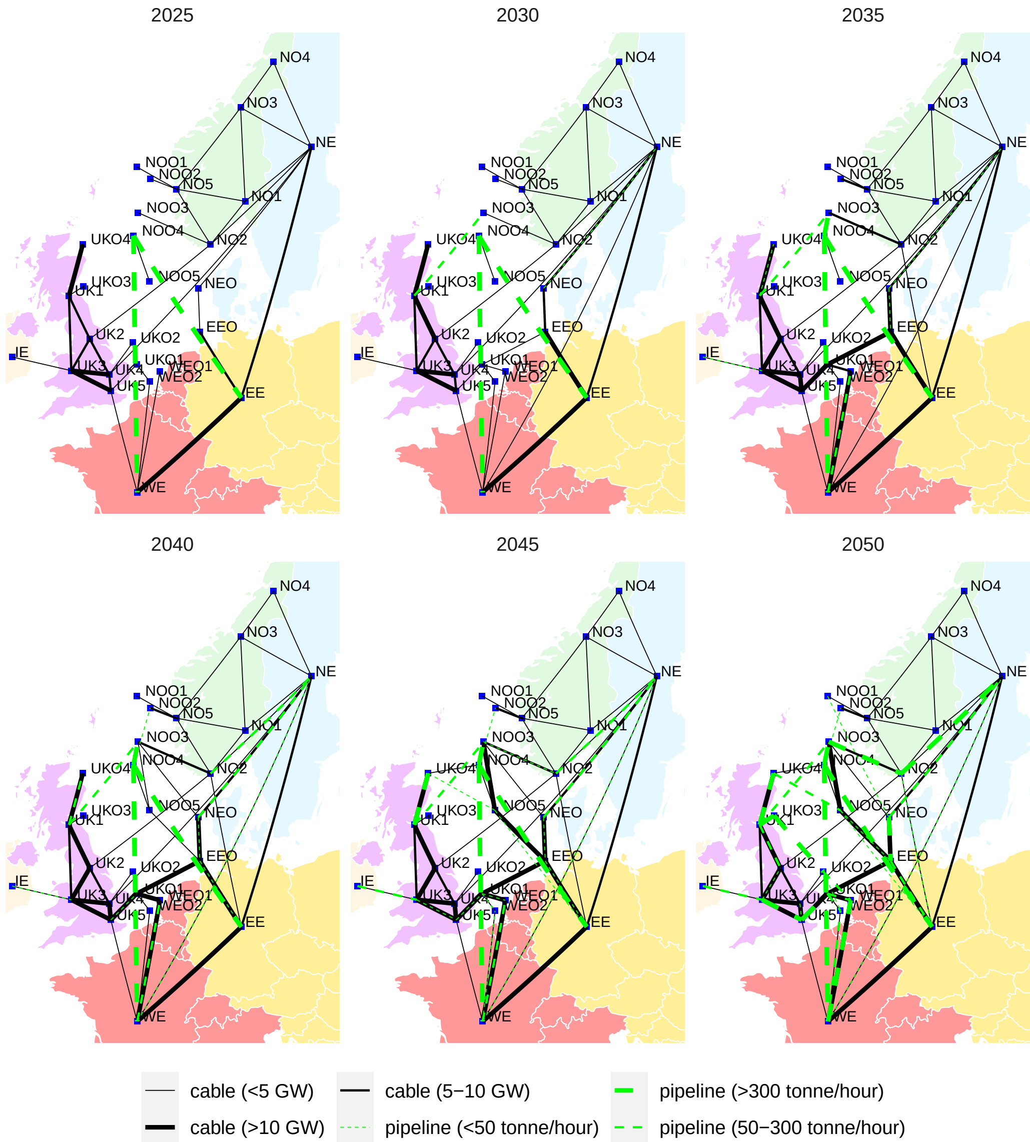

Figure 6: Expected solution of the grid design towards 2050 (REORIENT model).

in UK4-UK5. By 2050, the line NEO-EEO will have 44.90 GW capacity in REORIENT model compared with 36.81 GW in its counterpart. NOO3-NEO presents a significant difference as well with 4.4 GW capacity in REORIENT model and 12.26 GW in the investment-only model by 2050. NOO2 and NOO3 are not connected in the REORIENT model but are connected in the other model.

By comparing Figures 7 and 8, we notice that in both models, NOO3 is an important offshore region which receives significant investment in offshore wind and electrolysers due to its location and high wind availability. A major difference is found in offshore wind capacity in NEO and UKO4. The REORIENT model has a higher investment in offshore wind in NEO in all investment steps.

Tables 8 and 9 present the accumulated capacity of each technology in each region offshore wind will surpass onshore wind and become the most important renewable power supply by 2050. In

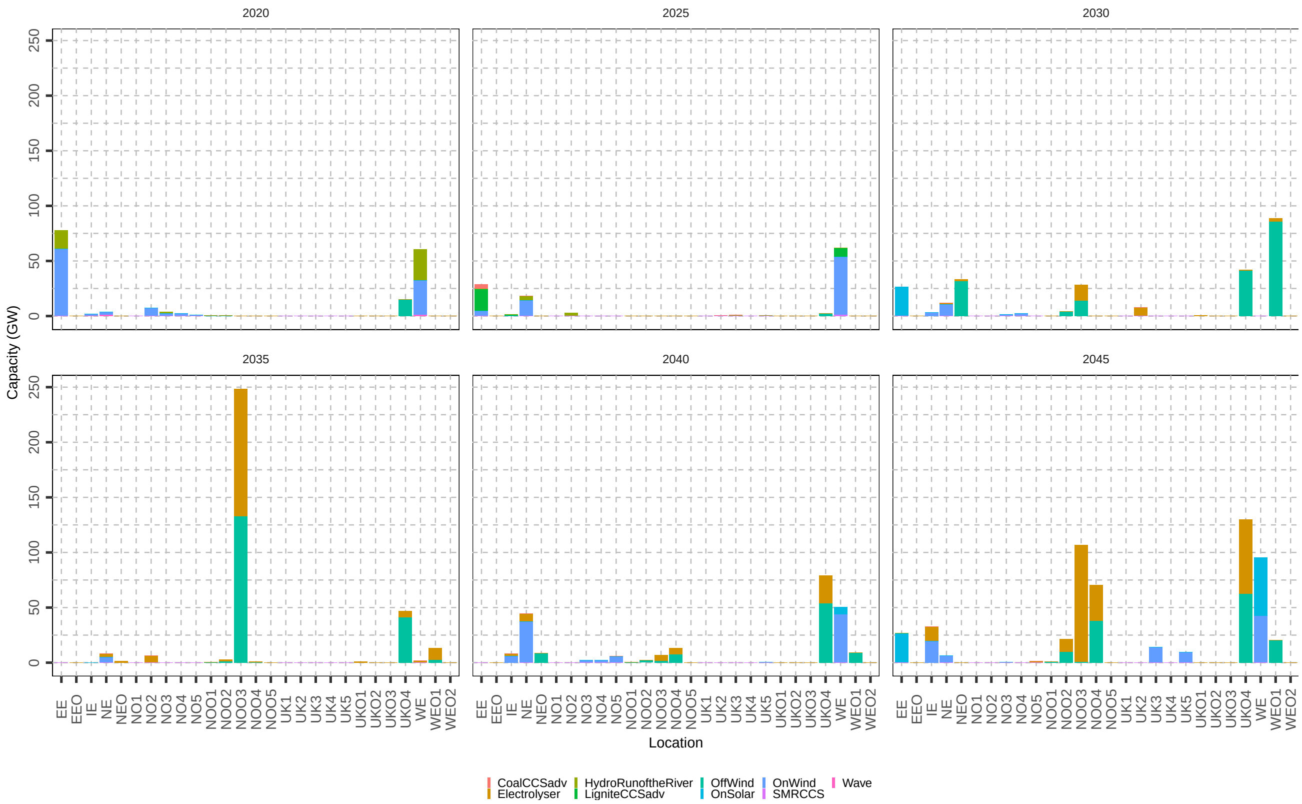

Figure 7: Expected investment decisions towards 2050 (investment only model).

Table 8: Results of accumulated capacity in Europe (investment-only model).

Year	Offshore wind (GW)	Onshore wind (GW)	Onshore solar (GW)	Electrolyser offshore (GW)	Electrolyser onshore (GW)	Transmission line (GW)	Hydrogen pipeline (ktonne/hour)
2025	35.72	279.24	119.83	0.00	0.00	148.66	0.00
2030	36.26	354.17	119.83	0.00	0.00	190.46	0.00
2035	212.08	364.02	146.29	12.46	8.66	586.61	0.73
2040	397.01	373.98	146.29	161.64	14.74	909.83	6.98
2045	465.95	355.11	150.86	174.57	20.51	985.28	7.80
2050	608.14	269.46	171.42	248.01	27.19	1084.87	15.70

Table 9: Results of accumulated capacity in Europe (REORIENT model).

Year	Offshore wind (GW)	Onshore wind (GW)	Onshore solar (GW)	Electrolyser offshore (GW)	Electrolyser onshore (GW)	Transmission line (GW)	Hydrogen pipeline (ktonne/hour)
2025	35.92	277.39	119.83	0.00	0.00	148.84	2.94
2030	38.33	348.67	119.83	0.00	0.00	190.73	3.19
2035	215.35	366.35	146.29	20.25	9.35	536.56	3.59
2040	394.34	371.60	146.29	156.90	20.38	904.63	6.19
2045	461.80	357.82	151.91	172.95	21.44	998.00	6.93
2050	593.89	293.15	171.42	253.37	24.85	1061.02	13.63

the investment-only model, more than 23 GW more transmission line capacity is needed by 2050 compared with the results using the REORIENT model. In both models, hydrogen is produced mainly from SMRCCS at the initial stages but gradually replaced by electrolysers. Also, both models decide to produce green hydrogen mainly offshore. The hydrogen pipeline capacity is lower in the REORIENT model compared with the counterpart by the end of the planning stage.

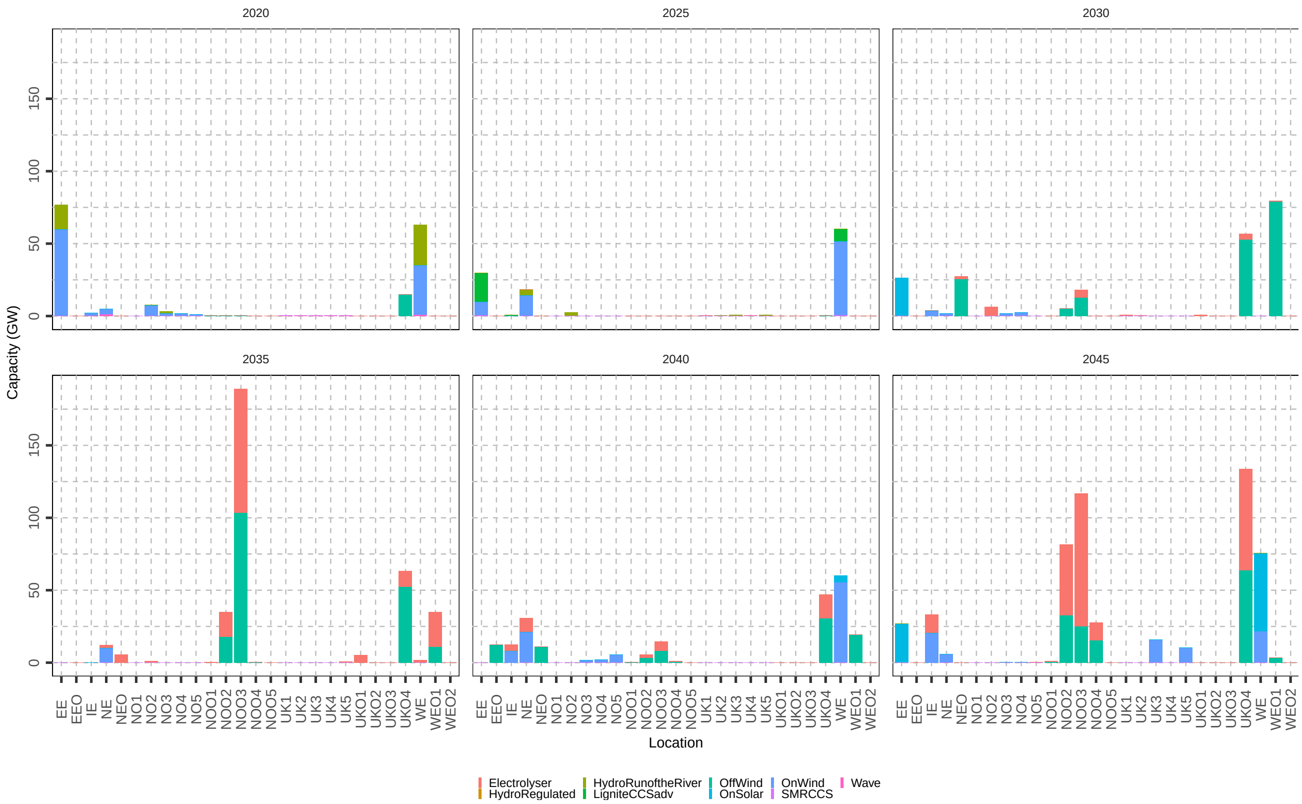

Figure 8: Expected investment decisions towards 2050 (REORIENT model).

In addition, the total cost over the given planning horizon is €1694.47 billion in the investment-only model and €1691.50 billion in the REORIENT model. Furthermore, the REORIENT yields 24% lower investment cost in the North Sea region compared with the traditional investment-only model. This shows the potential value of doing integrated planning. The value of REORIENT model can be further revealed once more retrofitting options are included, e.g., by including more existing natural gas pipelines.

7. Discussion

In this paper, we integrated investment, retrofit and abandonment planning in a multi-horizon stochastic MILP model. The model is generally applicable to studying a specific planning problem for a production plant or a large-scale energy system planning problem for a region.

We used the model to study the investment planning of a European energy system. We considered regional retrofit at a high level and conduct a techno-economical analysis. Unlike traditional retrofit models for process systems, we have omitted detailed modelling of the processes, which is a compromise due to the large scale of the study. The sensitivity analysis presented in this paper can be used as a benchmark for future studies.

In the case study, we find that although reducing retrofitting costs can trigger the retrofitting of some oil and gas infrastructures, it may not be a sufficiently strong incentive for platform retrofitting compared with pipeline retrofitting. This is because the loss of oil and gas profit is much larger than the reduction in retrofitting cost. Additionally, for platforms, a lot of investment needs to be made for producing green hydrogen upon removing the existing structure. Other driving factors, such as policies, are therefore needed to encourage oil and gas operators to retrofit their infrastructure or reduce production for the energy transition.

From an algorithm perspective, the proposed algorithm solved the problem instances efficiently. The problem instances have many regions and technologies and, therefore, are highly degenerate. The CP helps the proposed enhanced Benders algorithm to converge faster. In addition, the proposed enhanced Benders decomposition can be applied to a class of problems that can be formulated as Equations (10) and (9). Other strategies to accelerate Benders decomposition, including adding combinatorial cuts, trust region, local branching methods, and partial surrogate are tested. However, the improvement in performance is not significant.

There are some limitations of the case study: (1) in the case study, the offshore fields are aggregated into representative fields, which loses the modelling of the retrofit and abandonment for specific fields; (2) there are other parameters that may affect the investment decisions such as CO_2 budget can be an uncertain parameter and change the results. We believe that oil and gas prices have a more direct relation and economic trade-off with retrofit and abandonment decisions; therefore, we choose to consider oil and gas prices as the uncertain parameter, and (3) we only consider green and blue hydrogen. However, hydrogen produced by other means may also be relevant and affect the results. In addition, although the MHSP can include uncertainty from short-term and long-term time horizons more efficiently, uncertain parameters such as oil and gas prices can be affected by decisions taken. This can not be captured using MHSP. However, there have been modelling and computational strategies for multi-stage stochastic programming with endogenous and exogenous uncertainties (Goel & Grossmann, 2006; Apap & Grossmann, 2017). It may be possible to combine the approaches in (Goel & Grossmann, 2006; Apap & Grossmann, 2017) with MHSP to address this limitation.

8. Conclusions and future work

This paper has presented the REORIENT model, a multi-horizon stochastic MILP for integrated investment, retrofit and abandonment energy-system planning. The major novelties and contributions are: (1) we developed an MHSP model for integrated investment, retrofit and abandonment planning of energy systems, (2) we included uncertainty from both strategic and operational time horizons in such a model, (3) an enhanced Benders algorithm was developed to solve large-scale MILP faster and (4) the triggering parameters for retrofitting is investigated by conducting sensitivity analysis and a comparison between the REORIENT model and investment planning only model is made. Results from our case study indicate that: (1) for pipelines that are not in use, when the retrofitting cost is below 20% of the cost of building new ones, it is more economical to retrofit most of the pipelines than building new ones. For pipelines that transport natural gas, it is economical to be retrofitted in some natural gas price scenarios, (2) platform clusters keep producing oil and gas rather than being retrofitted for hydrogen use, and the clusters abandonment takes place at the last investment stage, (3) compared with an investment planning model, the REORIENT model yields €3 billion lower total cost, and 24% lower investment cost in the North Sea region, and (4) the proposed Benders algorithm can solve the model efficiently and is 6.8 times faster than the level set stabilised Benders decomposition which cannot solve the largest instance.

In the future, the REORIENT model can be used for more energy systems analysis, such as investigating the integrated planning for other regions, such as the continental shelf of the United States, or focusing on some specific platforms in a smaller region. In addition, other solution methods, such as Lagrangean type algorithms and progressive hedging algorithms, can be further developed for solving large-scale MHSP more efficiently. Furthermore, extending MHSP to manage endogenous uncertainty may be valuable in the future.

CRediT author statement

Hongyu Zhang: Conceptualisation, Methodology, Software, Validation, Formal analysis, Investigation, Visualisation, Data curation, Writing - original draft, Writing - review & editing. **Ignacio E. Grossmann:** Conceptualisation, Methodology, Supervision, Writing - review & editing. **Brage Rugstad Knudsen:** Conceptualisation, Methodology, Supervision, Writing - review & editing, Funding acquisition. **Ken McKinnon:** Conceptualisation, Methodology, Writing - review & editing. **Rodrigo Garcia Nava:** Conceptualisation, Methodology, Software. **Asgeir Tomasgard:** Conceptualisation, Methodology, Supervision, Writing - review & editing, Funding acquisition.

Declaration of competing interest

The authors declare that they have no known competing financial interests or personal relationships that could have appeared to influence the work reported in this paper.

Acknowledgements

This work was supported by the Research Council of Norway through PETROSENTER LowEmission [project code 296207].

References

van Ackooij, W., Frangioni, A., & de Oliveira, W. (2016). Inexact stabilized Benders' decomposition approaches with application to chance-constrained problems with finite support. *Computational Optimization and Applications*, *65*, 637–669. doi:10.1007/S10589-016-9851-Z/METRICS.

Apap, R. M., & Grossmann, I. E. (2017). Models and computational strategies for multistage stochastic programming under endogenous and exogenous uncertainties. *Computers & Chemical Engineering*, *103*, 233–274. doi:10.1016/J.COMPCHEMENG.2016.11.011.

Backe, S., Skar, C., del Granado, P. C., Turgut, O., & Tomasgard, A. (2022). EMPIRE: An open-source model based on multi-horizon programming for energy transition analyses. *SoftwareX*, *17*. doi:10.1016/j.softx.2021.100877.

Bakker, S., Vrålstad, T., & Tomasgard, A. (2019). An optimization model for the planning of offshore plug and abandonment campaigns. *Journal of Petroleum Science and Engineering*, *180*, 369–379. doi:10.1016/j.petrol.2019.05.042.

Bakker, S. J., Kleiven, A., Fleten, S. E., & Tomasgard, A. (2021a). Mature offshore oil field development: Solving a real options problem using stochastic dual dynamic integer programming. *Computers and Operations Research*, *136*. doi:10.1016/j.cor.2021.105480.

Bakker, S. J., Wang, A., & Gounaris, C. E. (2021b). Vehicle routing with endogenous learning: Application to offshore plug and abandonment campaign planning. *European Journal of Operational Research*, *289*, 93–106. doi:10.1016/j.ejor.2020.06.039.

Birge, J. R. (1985). Decomposition and Partitioning Methods for Multistage Stochastic Linear Programs. *https://doi.org/10.1287/opre.33.5.989*, *33*, 989–1007. doi:10.1287/OPRE.33.5.989.

Cho, S., Li, C., & Grossmann, I. E. (2022). Recent advances and challenges in optimization models for expansion planning of power systems and reliability optimization. *Computers & Chemical Engineering*, *165*, 107924. doi:10.1016/J.COMPCHEMENG.2022.107924.

Conejo, A. J., Baringo Morales, L., Kazempour, S. J., & Siddiqui, A. S. (2016). *Investment in electricity generation and transmission*. Springer Cham. doi:10.1007/978-3-319-29501-5.

Dunning, I., Huchette, J., & Lubin, M. (2017). JuMP: A modeling language for mathematical optimization. *SIAM Review*, *59*, 295–320. doi:10.1137/15M1020575.

Durakovic, G., del Granado, P. C., & Tomasgard, A. (2023). Powering Europe with North Sea offshore wind: The impact of hydrogen investments on grid infrastructure and power prices. *Energy*, *263*, 125654. doi:10.1016/J.ENERGY.2022.125654.

Escudero, L. F., Garín, M. A., & Unzueta, A. (2017). Scenario cluster Lagrangean decomposition for risk averse in multistage stochastic optimization. *Computers & Operations Research*, *85*, 154–171. doi:10.1016/J.COR.2017.04.007.

European Commission (2020). A European Green Deal. URL: https://commission.europa.eu/strategy-and-policy/priorities-2019-2024/european-green-deal_en [Accessed February 2023].

European Commission (2022). REPowerEU. URL: https://ec.europa.eu/commission/presscorner/detail/en/ip_22_3131 [Accessed February 2023].

Fleten, S.-E., Gunnerud, V., Hem, Ø. D. H., & Svendsen, A. (2011). Real option valuation of offshore petroleum field tie-ins. *Journal of Real Options*, . URL: https://ssrn.com/abstract=1992983. [Accessed February 2023].

Fodstad, M., Egging, R., Midthun, K., & Tomasgard, A. (2016). Stochastic modeling of natural gas infrastructure development in Europe under demand uncertainty. *Energy Journal*, *37*, 5–32. doi:10.5547/01956574.37.SI3.mfod.

Fors, T., Frank, H., & Christoph, B. (2021). *Hydrogen infrastructure-the pillar of energy transition*. Technical Report Siemens. URL: https://assets.siemens-energy.com/siemens/assets/api/uuid:3d4339dc-434e-4692-81a0-a55adbcaa92e/200915-whitepaper-h2-infrastructure-en.pdf [Accessed February 2023].

Galan, A., de Prada, C., Gutierrez, G., Sarabia, D., Grossmann, I. E., & Gonzalez, R. (2019). Implementation of RTO in a large hydrogen network considering uncertainty. *Optimization and Engineering*, *20*, 1161–1190. doi:10.1007/s11081-019-09444-3.

Gentile, V., Renaud-Bezot, C., & Simon, M. (2021). *Re-Stream – Study on the reuse of oil and gas infrastructure for hydrogen and CCS in Europe*. Technical Report Carbon Limits. URL: https://iogpeurope.org/wp-content/uploads/2022/01/Re-stream-final-report_Oct2021.pdf [Accessed February 2023].

Geoffrion, A. M., & Balakrishnan, V. (1972). Generalized Benders Decomposition. *Journal of Optimization Theory and Applications*, *10*. doi:doi.org/10.1007/BF00934810.

Goel, V., & Grossmann, I. E. (2004). A stochastic programming approach to planning of offshore gas field developments under uncertainty in reserves. *Computers and Chemical Engineering*, *28*, 1409–1429. doi:10.1016/j.compchemeng.2003.10.005.

Goel, V., & Grossmann, I. E. (2006). A Class of stochastic programs with decision dependent uncertainty. *Mathematical Programming*, *108*, 355–394. doi:10.1007/S10107-006-0715-7/METRICS.

Grossmann, I. E., Westerberg, A. W., & Biegler, L. T. (1987). *Retrofit design of processes*. Technical Report Carnegie Mellon University. URL: https://kilthub.cmu.edu/articles/journal_contribution/Retrofit_design_of_processes/6467396/1 [Accessed February 2023].

Gupta, V., & Grossmann, I. E. (2012). An efficient multiperiod MINLP model for optimal planning of offshore oil and gas field infrastructure. *Industrial and Engineering Chemistry Research*, *51*, 6823–6840. doi:10.1021/ie202959w.

Gupta, V., & Grossmann, I. E. (2014). Multistage stochastic programming approach for offshore oilfield infrastructure planning under production sharing agreements and endogenous uncertainties. *Journal of Petroleum Science and Engineering*, *124*, 180–197. doi:10.1016/j.petrol.2014.10.006.

Gurobi Optimization, LLC (2022). Gurobi optimizer reference manual. URL: https://www.gurobi.com [Accessed February 2023].

Harsh, M. G., Saderne, P., & Biegler, L. T. (1989). A mixed integer flowsheet optimization strategy for process retrofits—the debottlenecking problem. *Computers & Chemical Engineering*, *13*, 947–957. doi:10.1016/0098-1354(89)85067-7.

Höök, M., Hirsch, R., & Aleklett, K. (2009). Giant oil field decline rates and their influence on world oil production. *Energy Policy*, *37*, 2262–2272. doi:10.1016/j.enpol.2009.02.020.

Huang, Z., Zheng, Q. P., & Liu, A. L. (2022). A Nested Cross Decomposition Algorithm for Power System Capacity Expansion with Multiscale Uncertainties. *INFORMS Journal on Computing*, *34*. doi:10.1287/ijoc.2022.1177.

Iyer, R. R., Grossmann, I. E., Vasantharajan, S., & Cullick, A. S. (1998). Optimal planning and scheduling of offshore oil field infrastructure investment and operations. *Industrial & Engineering Chemistry Research*, *37*, 1380–1397. doi:doi.org/10.1021/ie970532x.

Jackson, J. R., & Grossmann, I. E. (2002). High-level optimization model for the retrofit planning of process networks. *Industrial and Engineering Chemistry Research*, *41*, 3762–3770. doi:10.1021/ie010699x.

Kaut, M., Midthun, K. T., Werner, A. S., Tomasgard, A., Hellemo, L., & Fodstad, M. (2014). Multi-horizon stochastic programming. *Computational Management Science*, *11*, 179–193. doi:10.1007/s10287-013-0182-6.

Kirui, K. B., Pichler, A., & Pflug, G. C. (2020). ScenTrees.jl: A Julia Package for Generating Scenario Trees and Scenario Lattices for Multistage Stochastic Programming. *Journal of Open Source Software*, *5*, 1912. doi:10.21105/JOSS.01912.

Krishnan, V., Ho, J., Hobbs, B. F., Liu, A. L., McCalley, J. D., Shahidehpour, M., & Zheng, Q. P. (2016). Co-optimization of electricity transmission and generation resources for planning and policy analysis: review of concepts and modeling approaches. *Energy Systems*, *7*, 297–332. doi:10.1007/S12667-015-0158-4/FIGURES/5.

Lara, C. L., Mallapragada, D. S., Papageorgiou, D. J., Venkatesh, A., & Grossmann, I. E. (2018). Deterministic electric power infrastructure planning: Mixed-integer programming model and nested decomposition algorithm. *European Journal of Operational Research*, *271*, 1037–1054. doi:10.1016/j.ejor.2018.05.039.

Lara, C. L., Siirola, J. D., & Grossmann, I. E. (2020). Electric power infrastructure planning under uncertainty: stochastic dual dynamic integer programming (SDDiP) and parallelization scheme. *Optimization and Engineering*, *21*, 1243–1281. doi:10.1007/s11081-019-09471-0.

Li, C., Conejo, A. J., Liu, P., Omell, B. P., Siirola, J. D., & Grossmann, I. E. (2022). Mixed-integer linear programming models and algorithms for generation and transmission expansion planning of power systems. *European Journal of Operational Research*, *297*, 1071–1082. doi:10.1016/j.ejor.2021.06.024.

Li, C., & Grossmann, I. E. (2019). A generalized Benders decomposition-based branch and cut algorithm for two-stage stochastic programs with nonconvex constraints and mixed-binary first and second stage variables. *Journal of Global Optimization*, *75*, 247–272. doi:10.1007/S10898-019-00816-8/TABLES/7.

Maggioni, F., Allevi, E., & Tomasgard, A. (2020). Bounds in multi-horizon stochastic programs. *Annals of Operations Research*, *292*, 605–625. doi:10.1007/S10479-019-03244-9/TABLES/5.

Magnanti, T. L., & Wong, R. T. (1981). Accelerating Benders Decomposition: Algorithmic Enhancement and Model Selection Criteria. *Operations Research*, *29*, 464–484. doi:10.1287/OPRE.29.3.464.

Mazzi, N., Grothey, A., McKinnon, K., & Sugishita, N. (2020). Benders decomposition with adaptive oracles for large scale optimization. *Mathematical Programming Computation*, . doi:10.1007/s12532-020-00197-0.

Munoz, F. D., Hobbs, B. F., & Watson, J. P. (2016). New bounding and decomposition approaches for MILP investment problems: Multi-area transmission and generation planning under policy constraints. *European Journal of Operational Research*, *248*, 888–898. doi:10.1016/j.ejor.2015.07.057.

Munoz, F. D., & Watson, J. P. (2015). A scalable solution framework for stochastic transmission and generation planning problems. *Computational Management Science*, *12*, 491–518. doi:10.1007/s10287-015-0229-y.

Neptune Energy (2023). PosHYdon pilot, Dutch North Sea. URL: https://www.neptuneenergy.com/esg/poshydon-hydrogen-pilot [Accessed February 2023].

Oliveira, F., Grossmann, I. E., & Hamacher, S. (2014). Accelerating Benders stochastic decomposition for the optimization under uncertainty of the petroleum product supply chain. *Computers & Operations Research*, *49*, 47–58. doi:10.1016/J.COR.2014.03.021.

Oliveira, F., Gupta, V., Hamacher, S., & Grossmann, I. E. (2013). A Lagrangean decomposition approach for oil supply chain investment planning under uncertainty with risk considerations. *Computers and Chemical Engineering*, *50*, 184–195. doi:10.1016/j.compchemeng.2012.10.012.

Pan, M., Smith, R., & Bulatov, I. (2013). A novel optimization approach of improving energy recovery in retrofitting heat exchanger network with exchanger details. *Energy*, *57*, 188–200. doi:10.1016/J.ENERGY.2012.10.056.

Pflug, G. C., & Pichler, A. (2015). Dynamic generation of scenario trees. *Computational Optimization and Applications*, *62*, 641–668. doi:10.1007/S10589-015-9758-0/FIGURES/5.

Philpott, A. B., Craddock, M., & Waterer, H. (2000). Hydro-electric unit commitment subject to uncertain demand. *European Journal of Operational Research*, *125*, 410–424. doi:10.1016/S0377-2217(99)00172-1.

Rossum, R. v. R., Jens, J., Guardia, G. L., Wang, A. W., Kühnen, L., & Overgaag, M. (2022). *European hydrogen backbone*. Technical Report European Hydrogen Backbone. URL: https://ehb.eu/files/downloads/ehb-report-220428-17h00-interactive-1.pdf [Accessed February 2023].

Schulze, T., & McKinnon, K. (2016). The value of stochastic programming in day-ahead and intra-day generation unit commitment. *Energy*, *101*, 592–605. doi:10.1016/j.energy.2016.01.090.

Schwartz, E., & Smith, J. E. (2000). Short-term variations and long-term dynamics in commodity prices. *Management Science*, *46*, 893–911. doi:10.1287/mnsc.46.7.893.12034.

Singh, K. J., Philpott, A. B., & Kevin Wood, R. (2009). Dantzig-wolfe decomposition for solving multistage stochastic capacity-planning problems. *Operations Research*, *57*, 1271–1286. doi:10.1287/opre.1080.0678.

Skar, C., Doorman, G. L., Pérez-Valdés, G. A., & Tomasgard, A. (2016). A multi-horizon stochastic programming model for the European power system. *Centre for Sustainable Energy Studies*, . URL: http://www.ntnu.no/documents/7414984/202064323/1_Skar_ferdig.pdf/855f0c3c-81db-440d-9f76-cfd91af0d6f0. [Accessed February 2023].

Steeger, G., & Rebennack, S. (2017). Dynamic convexification within nested Benders decomposition using Lagrangian relaxation: An application to the strategic bidding problem. *European Journal of Operational Research*, *257*, 669–686. doi:10.1016/J.EJOR.2016.08.006.

Støre, K., Fleten, S. E., Hagspiel, V., & Nunes, C. (2018). Switching from oil to gas production in a depleting field. *European Journal of Operational Research*, *271*, 710–719. doi:10.1016/j.ejor.2018.05.043.

Tong, D., Zhang, Q., Zheng, Y., Caldeira, K., Shearer, C., Hong, C., Qin, Y., & Davis, S. J. (2019). Committed emissions from existing energy infrastructure jeopardize 1.5 °C climate target. *Nature 2019 572:7769*, *572*, 373–377. doi:10.1038/s41586-019-1364-3.

Wallace, S. W., Helgesen, C., & Nystad, A. N. (1987). Generating production profiles for an-oil field*. *Mathematical Modelling*, (pp. 681–686). doi:doi.org/10.1016/0270-0255(87)90669-5.

Wang, Y., Pan, M., Bulatov, I., Smith, R., & Kim, J. K. (2012). Application of intensified heat transfer for the retrofit of heat exchanger network. *Applied Energy*, *89*, 45–59. doi:10.1016/J.APENERGY.2011.03.019.

Yee, T. F., & Grossmann, I. E. (1991). A screening and optimization approach for the retrofit of heat-exchanger networks. *Industrial & Engineering Chemistry Research*, *30*, 146–162. doi:doi.org/10.1021/ie00049a023.

You, F., & Grossmann, I. E. (2011). Multicut Benders decomposition algorithm for process supply chain planning under uncertainty. *Annals of Operations Research*, *210*, 191–211. doi:10.1007/S10479-011-0974-4.

Zhang, H., Mazzi, N., Mckinnon, K., Nava, R. G., & Tomasgard, A. (2022a). A stabilised Benders decomposition with adaptive oracles applied to investment planning of multi-region power systems with short-term and long-term uncertainty. *arXiv*, . doi:doi.org/10.48550/arXiv.2209.03471.

Zhang, H., Tomasgard, A., Knudsen, B. R., & Grossmann, I. E. (2022b). Offshore Energy Hubs in the Decarbonisation of the Norwegian Continental Shelf. In *ASME 2022 41st International Conference on Ocean, Offshore and Arctic Engineering*. American Society of Mechanical Engineers Digital Collection. doi:10.1115/OMAE2022-78551.

Zhang, H., Tomasgard, A., Knudsen, B. R., Svendsen, H. G., Bakker, S. J., & Grossmann, I. E. (2022c). Modelling and analysis of offshore energy hubs. *Energy*, *261*, 125219. doi:10.1016/j.energy.2022.125219.

Zverovich, V., Fábián, C. I., Ellison, E. F., & Mitra, G. (2012). A computational study of a solver system for processing two-stage stochastic LPs with enhanced Benders decomposition. *Mathematical Programming Computation*, *4*, 211–238. doi:10.1007/s12532-012-0038-z.

Appendix A. Nomenclature

Investment planning model indices and sets

$p \in \mathcal{P}$	set of technologies
$p \in \mathcal{P}^R$	set of candidate retrofit technologies
$p \in \mathcal{P}_p^R$	set of candidate technologies that an existing technology p can be retrofitted to ($p \in \mathcal{P}^R$) which including abandonment and prolong
$p \in \mathcal{P}^{RT}$	set of candidate technologies be retrofitted to
$i \in \mathcal{I}^{Ope}$	set of operational nodes
$i \in \mathcal{I}^{Inv}$	set of investment nodes
$j \in \mathcal{I}_i^{Inv}$	set of investment nodes j ($j \in \mathcal{I}^{Inv}$) succeed to investment node i ($i \in \mathcal{I}^{Inv}$)
$j \in \mathcal{I}_i^{Ope}$	set of operational nodes j ($j \in \mathcal{I}^{Ope}$) succeed to investment node i ($i \in \mathcal{I}^{Inv}$)
$(x, \theta, \lambda) \in \mathcal{F}_{i(k-1)}$	set of the Benders cut built up to iteration $k-1$, where x is the vector of sampled points, $theta$ and λ are the actually cost of subproblem at the sampled points, and the vector of subgradients at the sampled points, respectively.

Investment planning model parameters

C_{pi}^{InvV}	unitary investment cost of technology p in investment node i ($p \in \mathcal{P}, i \in \mathcal{I}^{Inv}$) [€/MW, €/MWh, €/kg]
C_{pi}^{InvF}	fixed capacity independent investment cost of technology p in investment node i ($p \in \mathcal{P}, i \in \mathcal{I}^{Inv}$) [€]
C_{pi}^{Fix}	unitary fix operational and maintenance cost of technology p in operational node i ($p \in \mathcal{P}, i \in \mathcal{I}^{Ope}$) [€/MW, €/MWh, €/kg]
C_{pi}^{ReTV}	unitary investment cost of retrofitted technology p in investment node i ($p \in \mathcal{P}^{RT}, i \in \mathcal{I}^{Inv}$) [€/MW, €/MWh, €/kg]
C_{pi}^{ReTF}	fixed capacity independent investment cost of retrofitted to technology p in investment node i ($p \in \mathcal{P}^{RT}, i \in \mathcal{I}^{Inv}$) [€]
$C^{ReTFixO}$	fix operational cost of the technology that is retrofitted to p in investment node i ($p \in \mathcal{P}^{RT}, i \in \mathcal{I}^{Inv}$) [€]
$C_{pi}^{ReFFixO}$	fix operational cost of retrofitted technology p in investment node i ($p \in \mathcal{P}^{RT}, i \in \mathcal{I}^{Inv}$) [€]
$X_{pi}^{MaxInv/MinInv}$	maximum/minimum built capacity of technology p in investment node i ($p \in \mathcal{P}, i \in \mathcal{I}^{Inv}$) [MW, MWh, kg]
X_p^{MaxAcc}	maximum installed capacity of technology over the planning horizon p ($p \in \mathcal{P}$) [MW, MWh, kg]
κ	scaling effect depending on time step between successive investment nodes
H_p	lifetime of technology p ($p \in \mathcal{P}$)
$X_{pi}^{HistReF}$	historical capacity of existing technology that can be retrofitted [MW, MWh, kg]
X_{pi}^{Hist}	historical capacity of technology p in operational node i ($p \in \mathcal{P}, i \in \mathcal{I}^{Ope}$) [MW, MWh, kg]
$X_{pi}^{MaxReT/MinReT}$	maximum/minimum built capacity of technology p in investment node i ($p \in \mathcal{P}^{RT}, i \in \mathcal{I}^{Inv}$) [MW, MWh, kg]
$X_{pi}^{MaxAccReT}$	maximum installed capacity of technology p ($p \in \mathcal{P}^{RT}$) [MW, MWh, kg]
x_i	right hand side of the operational problem
c_i	cost coefficients of the operational problem
$\pi_i^{Inv/Ope}$	discount factor multiplied probability of investment/operational node i, ($i \in \mathcal{I}^{Inv}/i \in \mathcal{I}^{Ope}$)
μ_i^E	CO_2 budget at operational node i ($i \in \mathcal{I}^{Ope}$)
μ_i^{DP}	scaling factor on power demand at operational node i ($i \in \mathcal{I}^{Ope}$)
μ_i^P	scaling factor on oil and gas production at operational node i ($i \in \mathcal{I}^{Ope}$)
μ_i^{DHy}	scaling factor on hydrogen demand at operational node i ($i \in \mathcal{I}^{Ope}$)
C_i^{CO2}	CO_2 emission price at operational node i ($i \in \mathcal{I}^{Ope}$)
$\mathcal{S}_i^{Ope}$	strategic stage of operational node i ($i \in \mathcal{I}^{Ope}$)
$\mathcal{S}_i^{Inv}$	strategic stage of investment node i ($i \in \mathcal{I}^{Inv}$)

Investment planning model variables

x_{pi}^{Acc}	accumulated capacity of device p in operational node i ($p \in \mathcal{P}, i \in \mathcal{I}^{Ope}$) [MW, MWh, kg]
x_{pi}^{Inv}	newly invested capacity of device p in investment node i_0 ($p \in \mathcal{P}, i \in \mathcal{I}^{Inv}$) [MW, MWh, kg]
y_{pi}^{Inv}	1 if technology p is newly invested in investment node i, 0 otherwise ($p \in \mathcal{P}, i \in \mathcal{I}^{Inv}$)
y_{pi}^{ReT}	1 if technology p is retrofitted to in investment node i, 0 otherwise ($p \in \mathcal{P}^{RT}, i \in \mathcal{I}^{Inv}$)
x_{pi}^{AccReT}	accumulated capacity of technology p that is retrofitted to in operational node i ($p \in \mathcal{P}^{RT}, i \in \mathcal{I}^{Ope}$)
y_{pi}^{ReF}	1 if technology p is retrofitted from in investment node i, 0 otherwise ($p \in \mathcal{P}^R, i \in \mathcal{I}^{Inv}$)
x_{pi}^{AccReF}	accumulated capacity of retrofitted from technology in operational node i ($p \in \mathcal{P}^R, i \in \mathcal{I}^{Ope}$)
x_{pi}^{ReT}	in operational node i ($p \in \mathcal{P}^R, i \in \mathcal{I}^{Ope}$)
c^{INV}	total investment and fixed operating and maintenance costs [€]
c_i^{OPE}	approximated operational cost in operational node i in Benders decomposition ($i \in \mathcal{I}^{Ope}$) [€]

Operational model indices and sets

$n \in \mathcal{N}$	set of time slices
$t \in \mathcal{T}$	set of hours in all time slices
$t \in \mathcal{T}_n$	set of hours in time slice n ($n \in \mathcal{N}$)
$l \in \mathcal{L}$	set of transmission lines
$l \in \mathcal{L}^{Hy}$	set of hydrogen pipelines
$l \in \mathcal{L}_z^{Out/In}$	set of transmission lines go out of/into region z
$l \in \mathcal{L}_z^{HyOut/HyIn}$	set of hydrogen pipelines go out of/into region z
$g \in \mathcal{G}$	set of thermal generation
$r \in \mathcal{G}^R$	set of renewable generation
$g \in \mathcal{G}^H$	set of hydropower generation including run of the river $\mathcal{G}^{HRor}$ and seasonal $\mathcal{G}^{HSea}$
$s \in \mathcal{S}^E$	set of electricity storage
$s \in \mathcal{S}^{Hy}$	set of hydrogen storage
$b \in \mathcal{B}^E$	set of electric boilers
$r \in \mathcal{R}$	set of SMRCCS
$e \in \mathcal{E}$	set of electrolysers
$f \in \mathcal{F}$	set of fuel cells
$z \in \mathcal{Z}^P$	set of all platform clusters
$z \in \mathcal{Z}$	set of all locations
$p \in \mathcal{P}^*$	set of all thermal generators, electric boilers, electrolysers, electricity storage, fuel cells and seasonal hydropower generation ($\mathcal{P}^* = \mathcal{G} \cup \mathcal{B}^E \cup \mathcal{E} \cup \mathcal{S}^E \cup \mathcal{F} \cup \mathcal{G}^{HSea}$)
$v \in \mathcal{V}^*$	set of hydrogen storage and SMRCCS plants ($\mathcal{V}^* = \mathcal{S}^{Hy} \cup \mathcal{R}$)

Operational model parameters

μ^E	CO_2 emission limit (tonne)
$\mu^{DP/DH/DHy}$	scaling effect on power demand/heat demand/hydrogen demand
H_t	number of hour(s) in one operational period t
π_t	weighted length of one operational period t
R_{rt}^{GR}	capacity factor of renewable unit r in period t ($r \in \mathcal{R}, t \in \mathcal{T}$)
η^*	efficiency of electric boilers, fuel cells, thermal generators, electric storage and transmission lines $* = \{\text{BE, SE, L, HrG}\}$ indexed by related sets
E_g^G	CO_2 emission factor of thermal generation g ($g \in \mathcal{G}$) [t/MWh]
C_g^G	total operational cost of generating 1 MW power from thermal generation g ($g \in \mathcal{G}$) [€/MW]
$C^{Shed,l}$	load shed penalty cost of power ($l = P$), heat ($l = H$) and hydrogen $l = Hy$ [€/MW, €/kg]
σ_z^{Res}	spinning reserve factor in region z ($z \in \mathcal{Z}$)
α_g^G	maximum ramp rate of generators ($g \in \mathcal{G}$) [MW/MW]
ρ^E	conversion factor of electrolyser to hydrogen [MWh/kg]
$P_{zt}^{DP/DH}$	power demand/heat demand in location z period t ($z \in \mathcal{Z}, t \in \mathcal{T}$) [MW]
ρ^F	hydrogen consumption factor of fuel cell [kg/MW]
P_g^{AccG}	accumulated capacity of thermal generator g ($g \in \mathcal{G}$) [MW]
$P_g^{AccHRor}$	accumulated capacity of run of the river hydropower generation g ($g \in \mathcal{G}^{HRor}$) [MW]
P_g^{Acc}	accumulated capacity of technology p ($p \in \mathcal{P}^*$) [MW]
Q_s^{AccSE}	accumulated storage capacity of electricity store s ($s \in \mathcal{S}^E$) [MWh]
P_l^{AccL}	accumulated capacity of line l ($l \in \mathcal{L}$) [MW]
C^R	operational cost of producing 1 kg hydrogen from SMRCCS [€/kg]
$P_{gt}^{HSea/HRor}$	production profile of seasonal hydropower/run of the river hydropower in location z period t ($z \in \mathcal{Z}, t \in \mathcal{T}$) [MW]
V_{zt}^{DHy}	hydrogen demand in region z period t ($z \in \mathcal{Z}, t \in \mathcal{T}$) [MW]
E^R	emission factor of SMRCCS
V^{Acc}	storage level, injection and withdrawal capacities of hydrogen storage and capacity of SMRCCS [kg]

Operational model variables

p_{gt}^G	power generation of thermal generator g in period t ($g \in \mathcal{G}, t \in \mathcal{T}$) [MW]
p_{gt}^{ResG}	power reserved of thermal generator g for spinning reserve requirement in period t ($g \in \mathcal{G}, t \in \mathcal{T}$) [MW]
$p_{st}^{SE+}/p_{st}^{SE-}$	charge/discharge power of electricity store s in period t ($s \in \mathcal{S}^E, t \in \mathcal{T}$) [MW]
p_{st}^{ResSE}	power reserved in electricity store s for spinning reserve requirement in period t ($s \in \mathcal{S}^E, t \in \mathcal{T}$) [MW]
q_{st}^{SE}	energy level of electricity store s at the start of period t ($s \in \mathcal{S}^E, t \in \mathcal{T}$) [MWh]
$p_{zt}^{GShed,l}$	generation shed for power ($l = P$) and heat ($l = H$) in location z in period t ($z \in \mathcal{Z}, t \in \mathcal{T}$) [MW]
$p_{zt}^{Shed,l}$	load shed for power ($l = P$) and heat ($l = H$) in location z in period t ($z \in \mathcal{Z}, t \in \mathcal{T}$) [MW]
$v_{zt}^{GShedHy}$	hydrogen production shed in location z in period t ($z \in \mathcal{Z}, t \in \mathcal{T}$) [kg]
v_{zt}^{ShedHy}	hydrogen load shed in location z in period t ($z \in \mathcal{Z}, t \in \mathcal{T}$) [kg]

p_{lt}^{L}	power flow in line l in period t ($l \in \mathcal{L}, t \in \mathcal{T}$) [MW]
p_{bt}^{BE}	power consumption of electric boiler b in period t ($b \in \mathcal{B}^{E}, t \in \mathcal{T}$) [MW]
p_{ft}^{F}	power generation of fuel cell f in period t ($f \in \mathcal{F}, t \in \mathcal{T}$) [MW]
p_{et}^{E}	power consumption of electrolyser e in period t ($e \in \mathcal{E}, t \in \mathcal{T}$) [MW]
$v_{st}^{SHy+}/v_{st}^{SHy-}$	injection/withdraw of hydrogen to (from) hydrogen storage s in period t ($s \in \mathcal{S}^{Hy}, t \in \mathcal{T}$) [kg]
v_{st}^{SHy}	storage level of hydrogen storage s in period t ($s \in \mathcal{S}^{Hy}, t \in \mathcal{T}$) [kg]
v_{rt}^{R}	hydrogen production of SMRCCS r in period t ($r \in \mathcal{R}, t \in \mathcal{T}$) [kg]
v_{lt}^{LHy}	hydrogen flow in pipeline l period t ($l \in \mathcal{L}^{Hy}, t \in \mathcal{T}$)
v_{vt}	hydrogen injection, withdraw, storage level of hydrogen storage, and hydrogen production of SMRCCS in period t ($v \in \mathcal{S}^{Hy} \cup \mathcal{R}$) [kg]